

计算视觉与模式识别

灰度变换与空间域滤波

$$g(x, y) = T[f]$$

其中

$$g, f : (R, R) \mapsto R$$

灰度变换

$$s = T(r)$$

其中

$$s = g(x, y)$$

$$r = f(x, y)$$

$$g(x, y) = T(f(x, y))$$

示例1

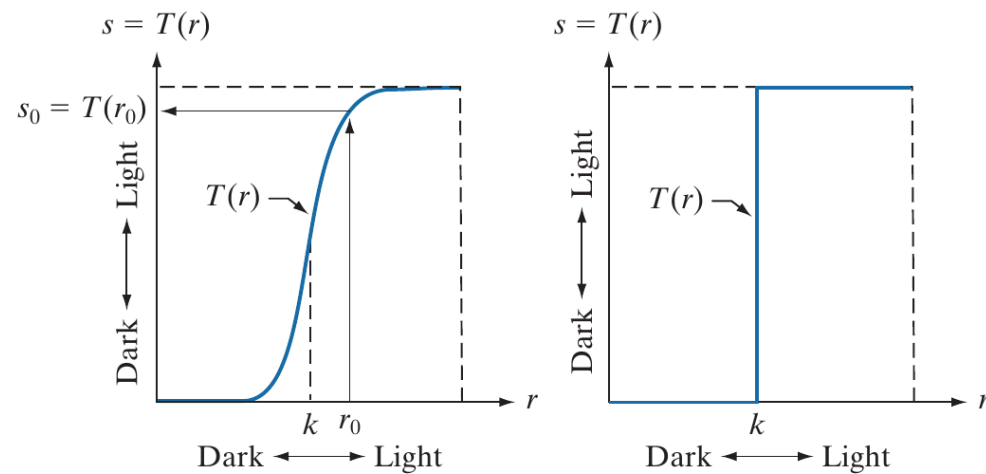
a b

FIGURE 3.2

Intensity transformation functions.

(a) Contrast stretching function.

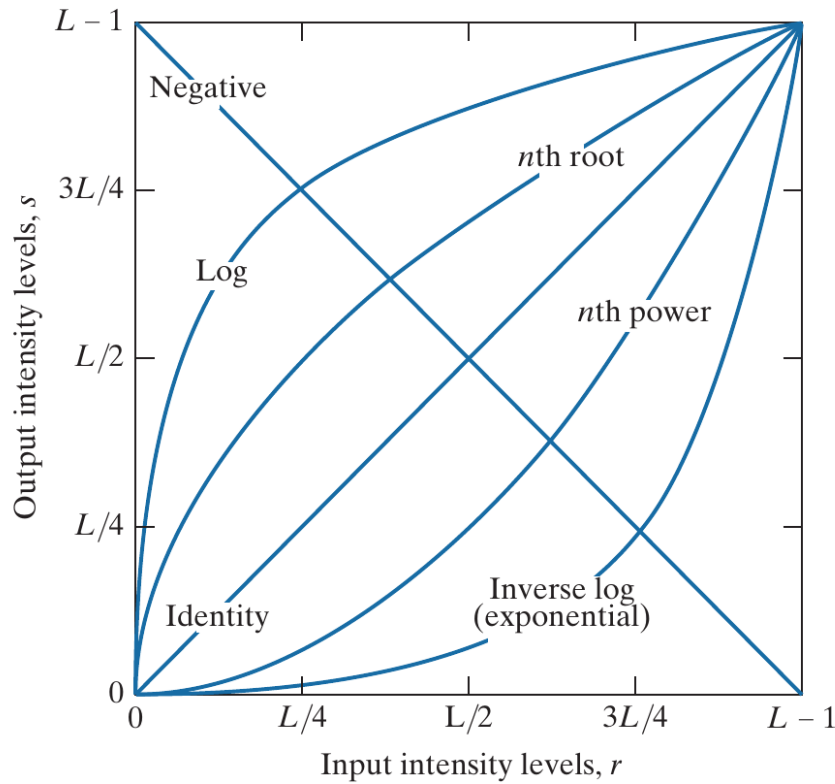
(b) Thresholding function.



示例2

FIGURE 3.3

Some basic intensity transformation functions. Each curve was scaled *independently* so that all curves would fit in the same graph. Our interest here is on the *shapes* of the curves, not on their relative values.

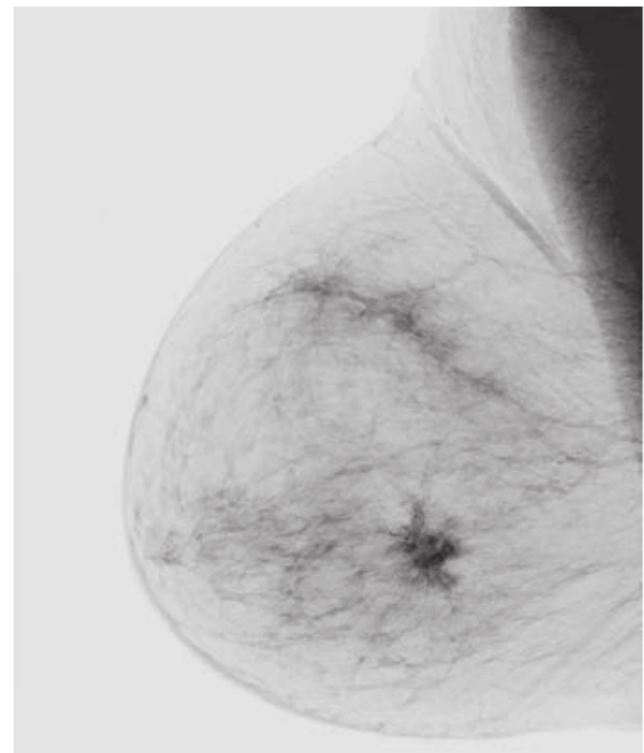
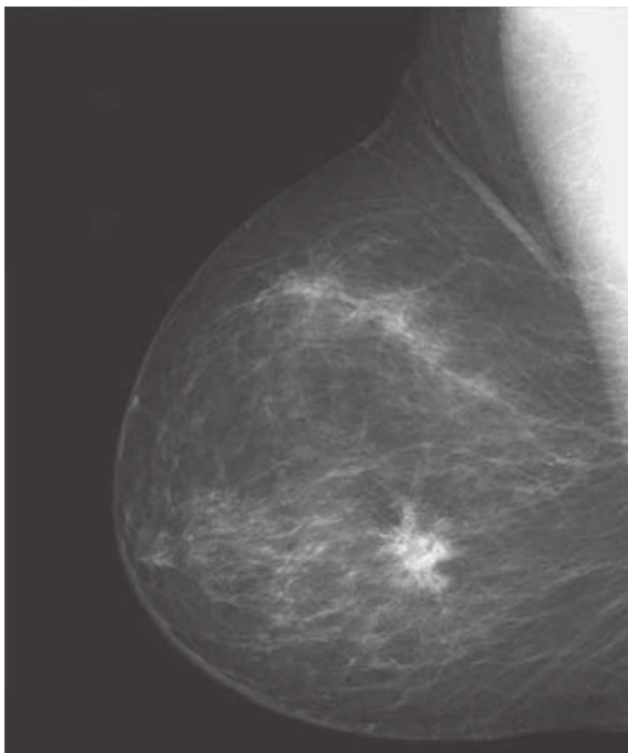


$$s = L - 1 - r$$

a b

FIGURE 3.4

(a) A digital mammogram.
(b) Negative image obtained using Eq. (3-3).
(Image (a)
Courtesy of
General Electric
Medical Systems.)

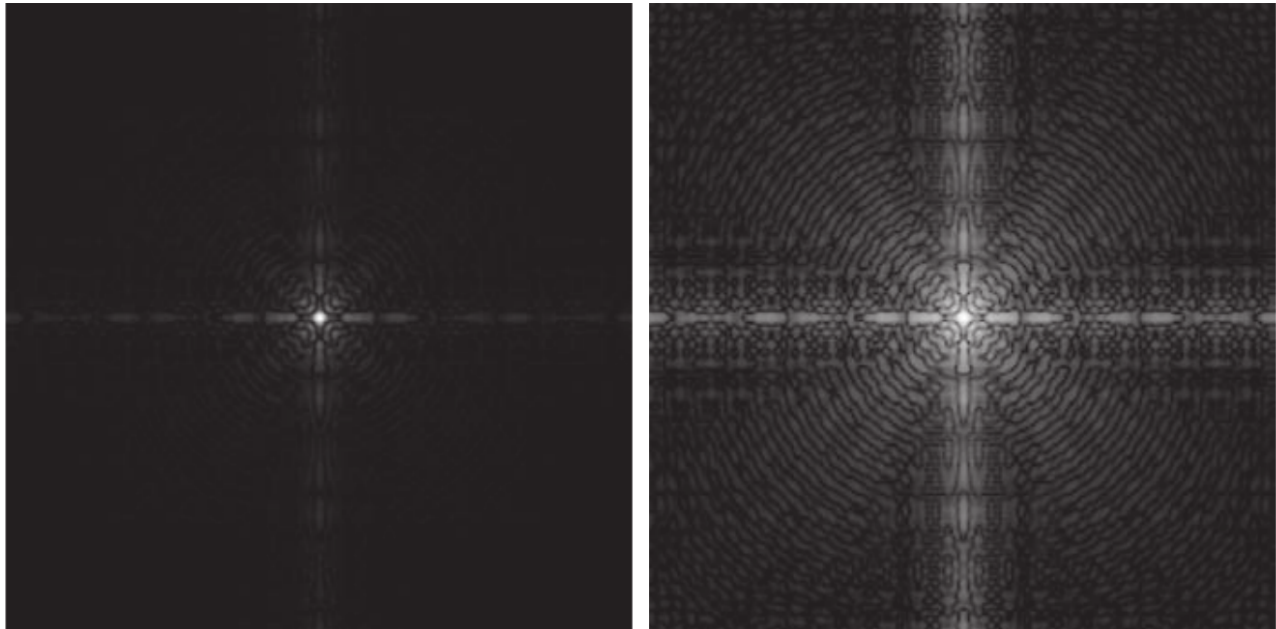


$$s = \ln(1 + r)$$

a b

FIGURE 3.5

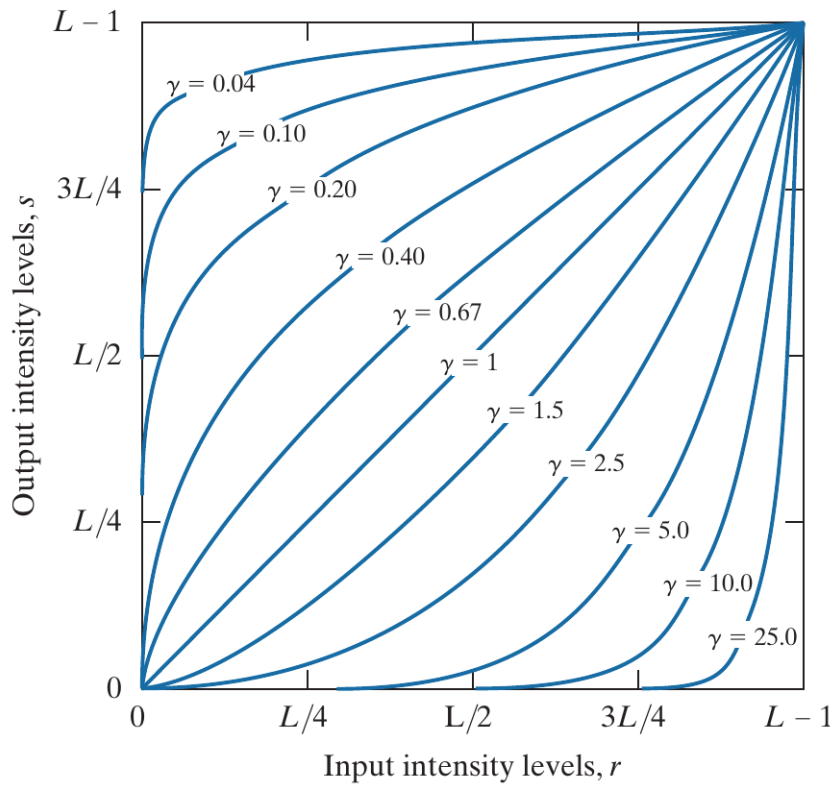
(a) Fourier spectrum displayed as a grayscale image.
(b) Result of applying the log transformation in Eq. (3-4) with $c = 1$. Both images are scaled to the range $[0, 255]$.



$$s = cr^\gamma$$

FIGURE 3.6

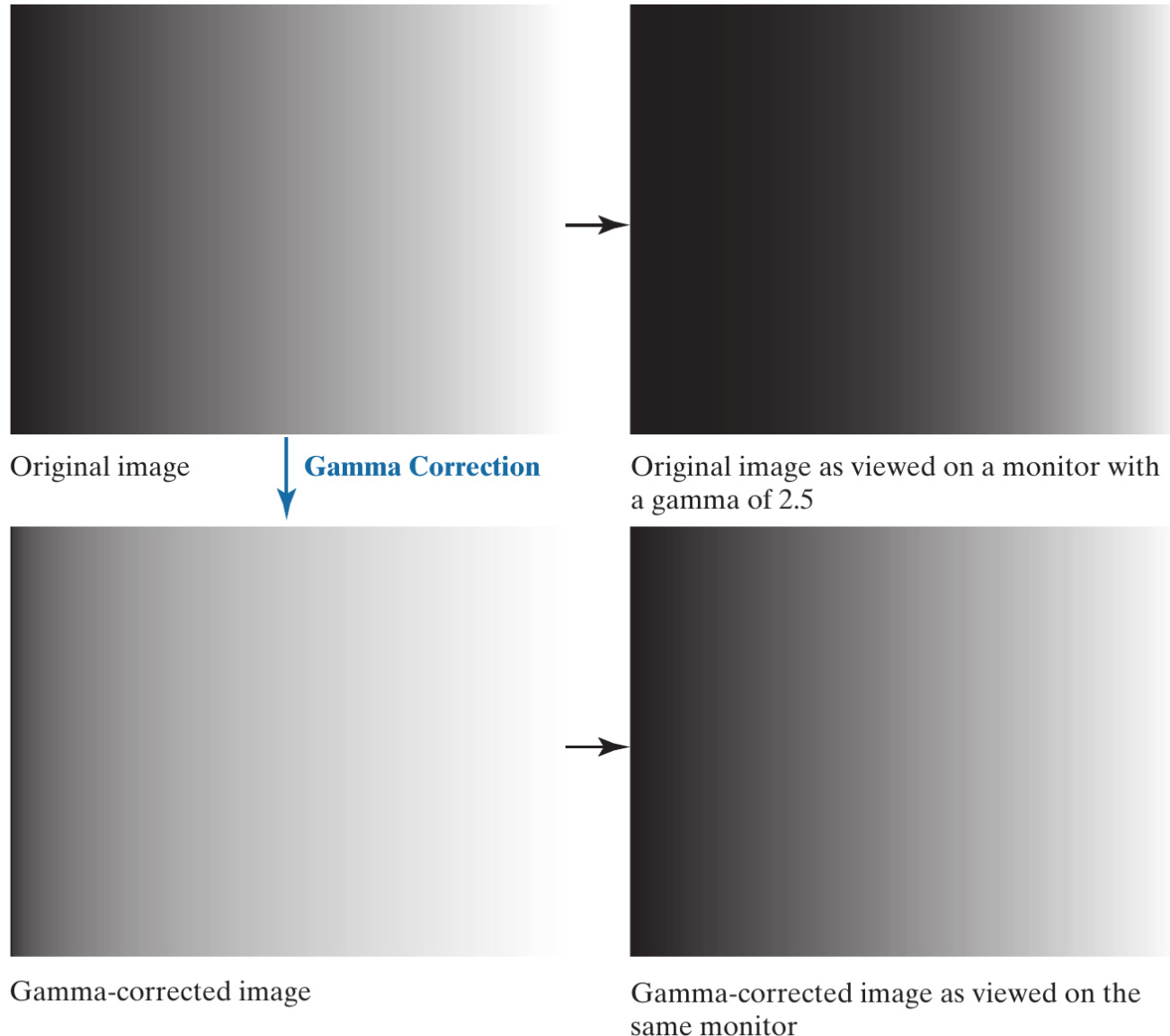
Plots of the gamma equation $s = cr^\gamma$ for various values of γ ($c = 1$ in all cases). Each curve was scaled independently so that all curves would fit in the same graph. Our interest here is on the *shapes* of the curves, not on their relative values.



a b
c d

FIGURE 3.7

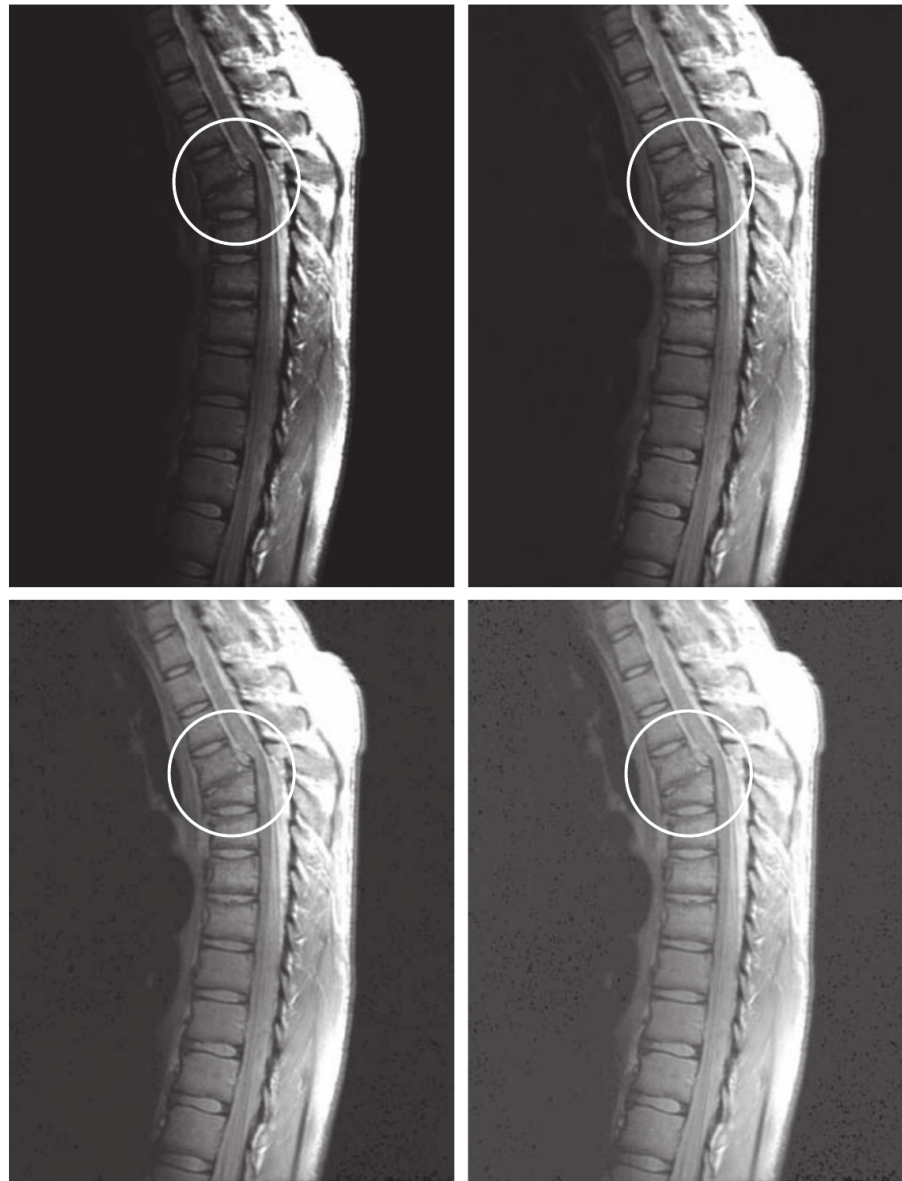
(a) Intensity ramp image. (b) Image as viewed on a simulated monitor with a gamma of 2.5. (c) Gamma-corrected image. (d) Corrected image as viewed on the same monitor. Compare (d) and (a).



a b
c d

FIGURE 3.8

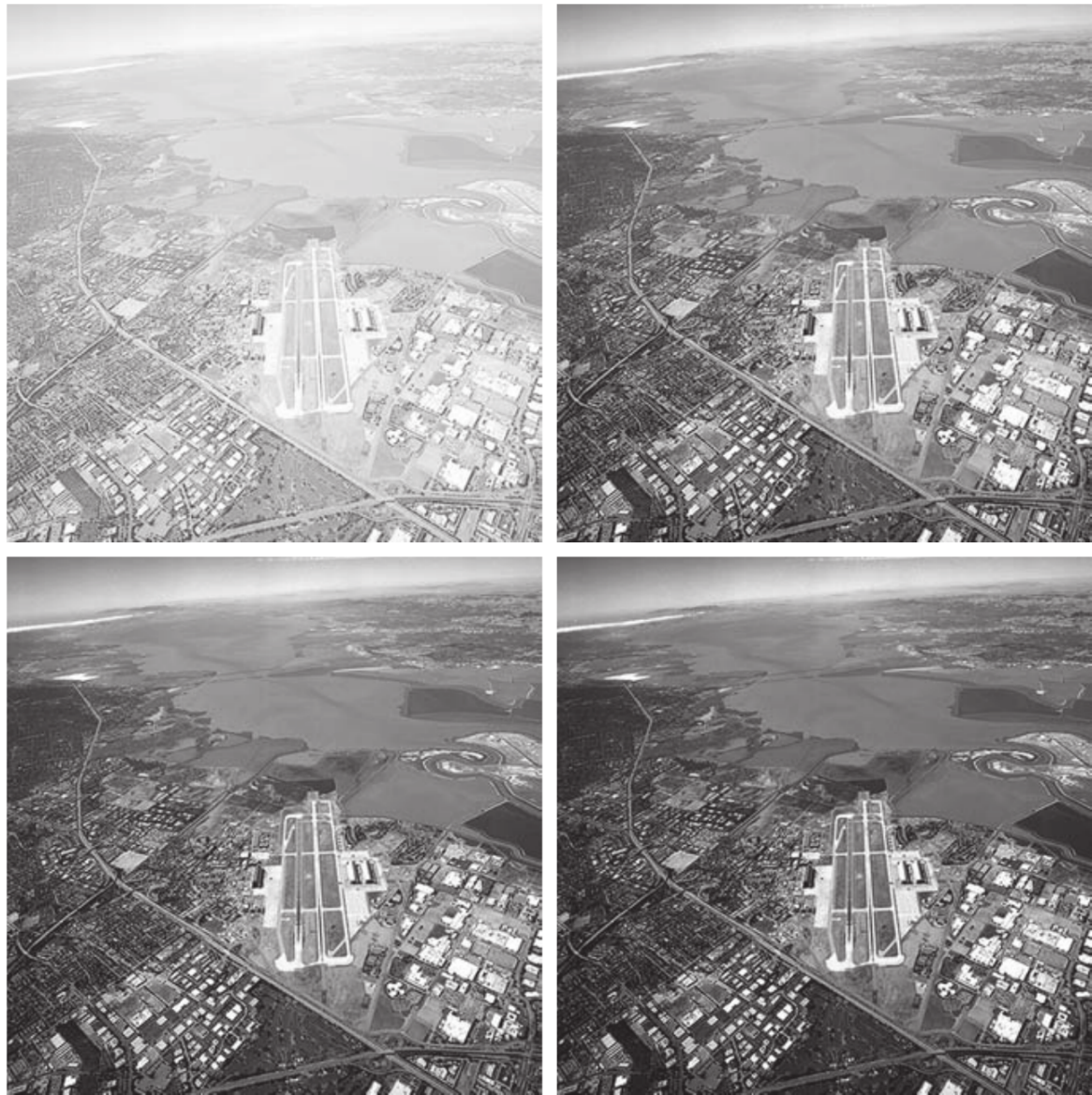
(a) Magnetic resonance image (MRI) of a fractured human spine (the region of the fracture is enclosed by the circle).
(b)–(d) Results of applying the transformation in Eq. (3-5) with $c = 1$ and $\gamma = 0.6, 0.4$, and 0.3 , respectively.
(Original image courtesy of Dr. David R. Pickens, Department of Radiology and Radiological Sciences, Vanderbilt University Medical Center.)



a b
c d

FIGURE 3.9

(a) Aerial image.
(b)–(d) Results
of applying the
transformation in
Eq. (3-5) with
 $\gamma = 3.0, 4.0,$ and
 $5.0,$ respectively.
($c = 1$ in all cases.)
(Original image
courtesy of
NASA.)



a b
c d

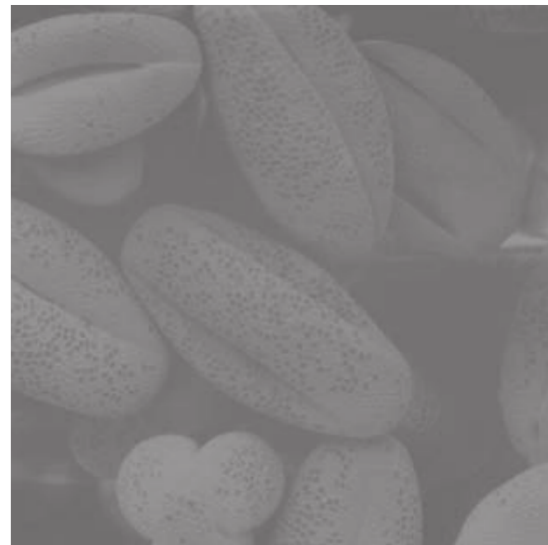
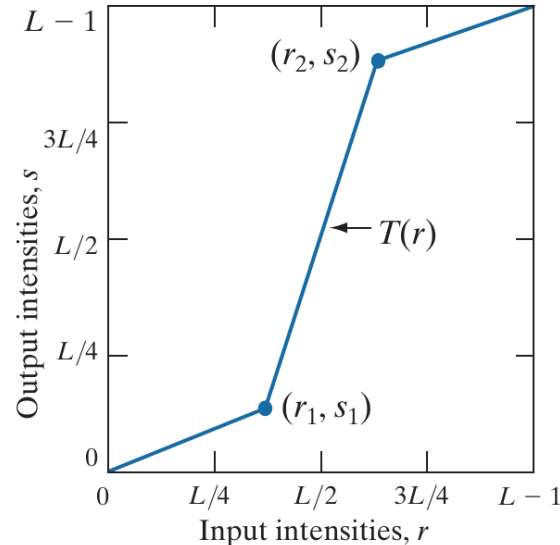
FIGURE 3.10

Contrast stretching.
(a) Piecewise linear transformation function. (b) A low-contrast electron microscope image of pollen, magnified 700 times.

(c) Result of contrast stretching.

(d) Result of thresholding.

(Original image courtesy of Dr. Roger Heady, Research School of Biological Sciences, Australian National University, Canberra, Australia.)

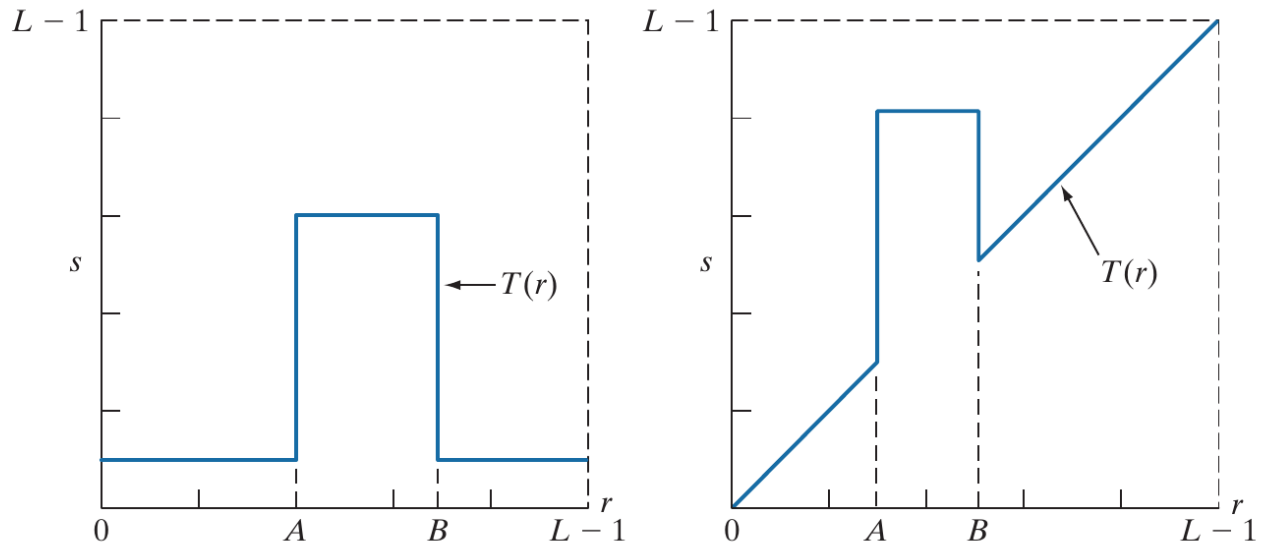


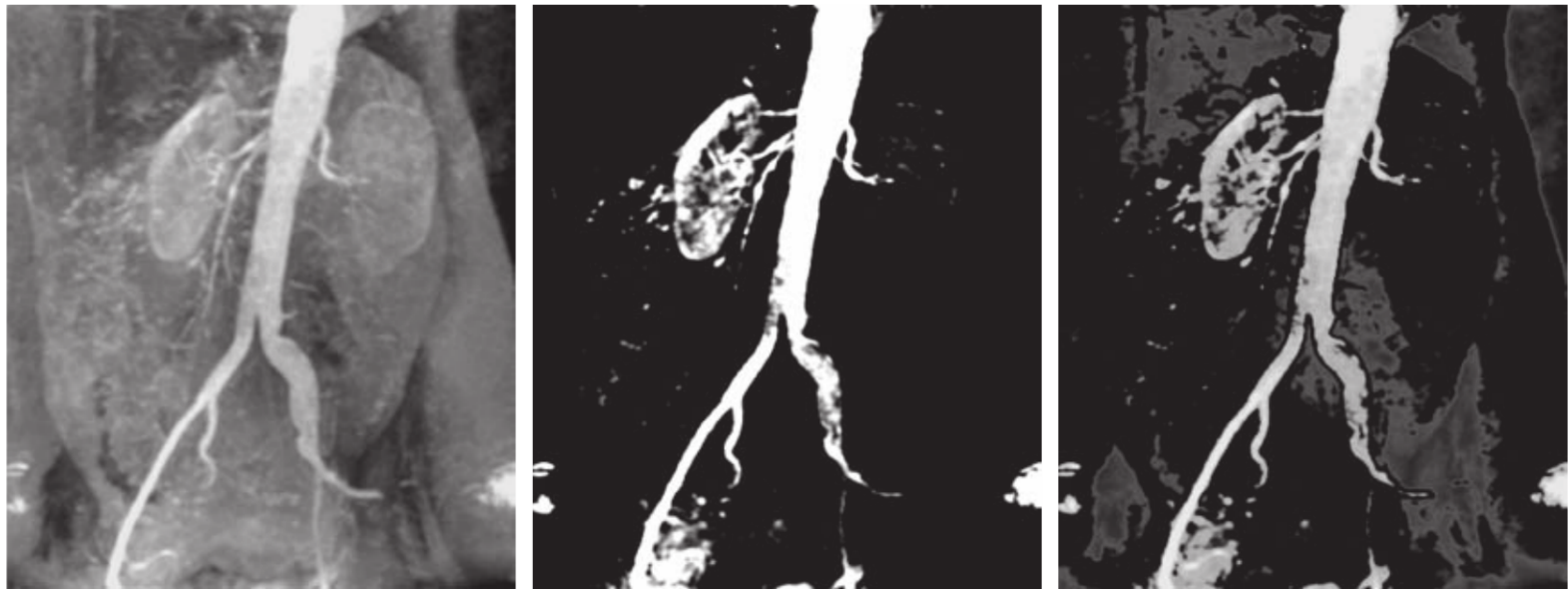
亮度分层

a b

FIGURE 3.11

- (a) This transformation function highlights range $[A, B]$ and reduces all other intensities to a lower level.
(b) This function highlights range $[A, B]$ and leaves other intensities unchanged.



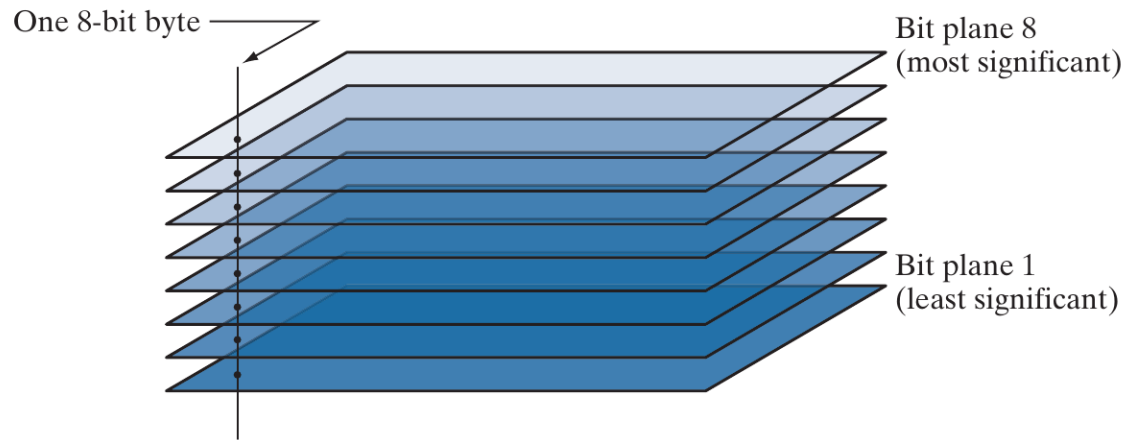


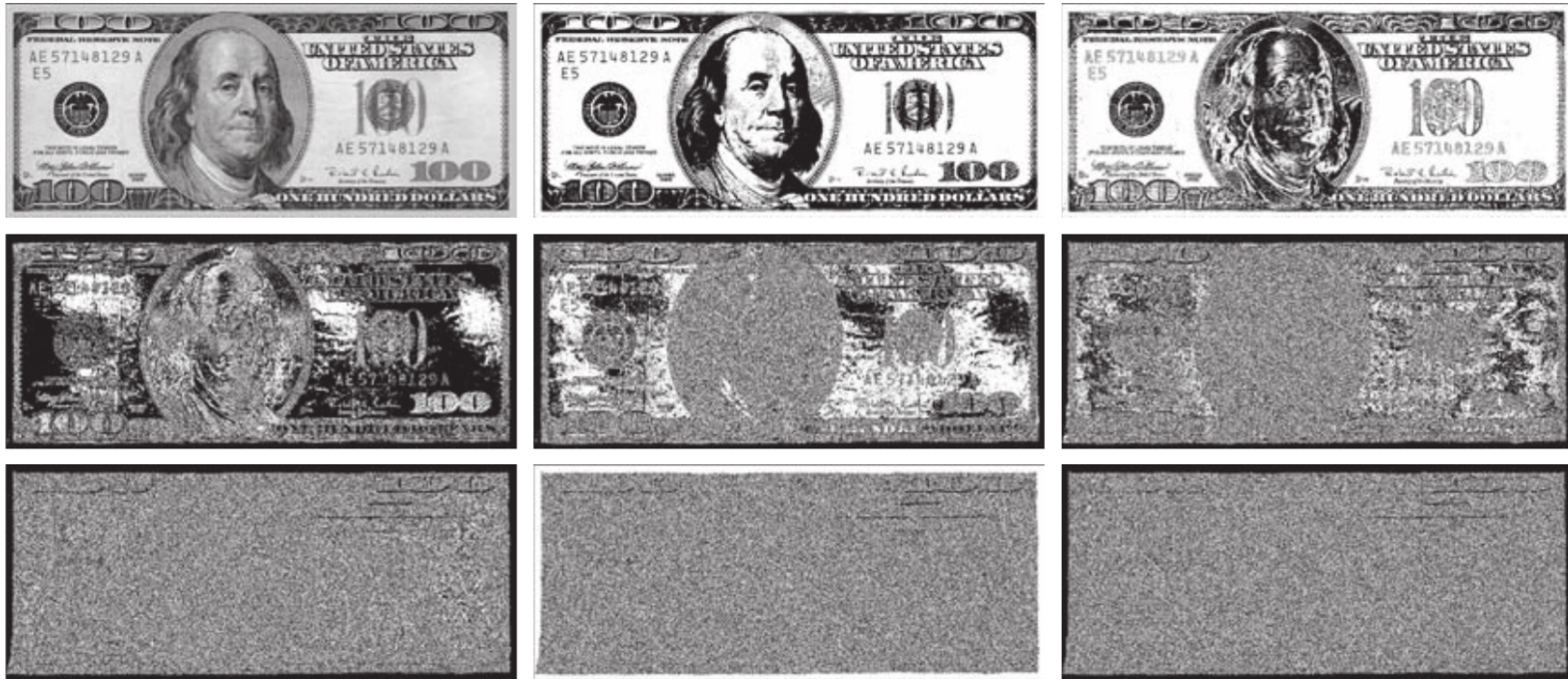
a b c

FIGURE 3.12 (a) Aortic angiogram. (b) Result of using a slicing transformation of the type illustrated in Fig. 3.11(a), with the range of intensities of interest selected in the upper end of the gray scale. (c) Result of using the transformation in Fig. 3.11(b), with the selected range set near black, so that the grays in the area of the blood vessels and kidneys were preserved. (Original image courtesy of Dr. Thomas R. Gest, University of Michigan Medical School.)

FIGURE 3.13

Bit-planes of an 8-bit image.





a	b	c
d	e	f
g	h	i

FIGURE 3.14 (a) An 8-bit gray-scale image of size 550×1192 pixels. (b) through (i) Bit planes 8 through 1, with bit plane 1 corresponding to the least significant bit. Each bit plane is a binary image..



a b c

FIGURE 3.15 Image reconstructed from bit planes: (a) 8 and 7; (b) 8, 7, and 6; (c) 8, 7, 6, and 5.

直方图

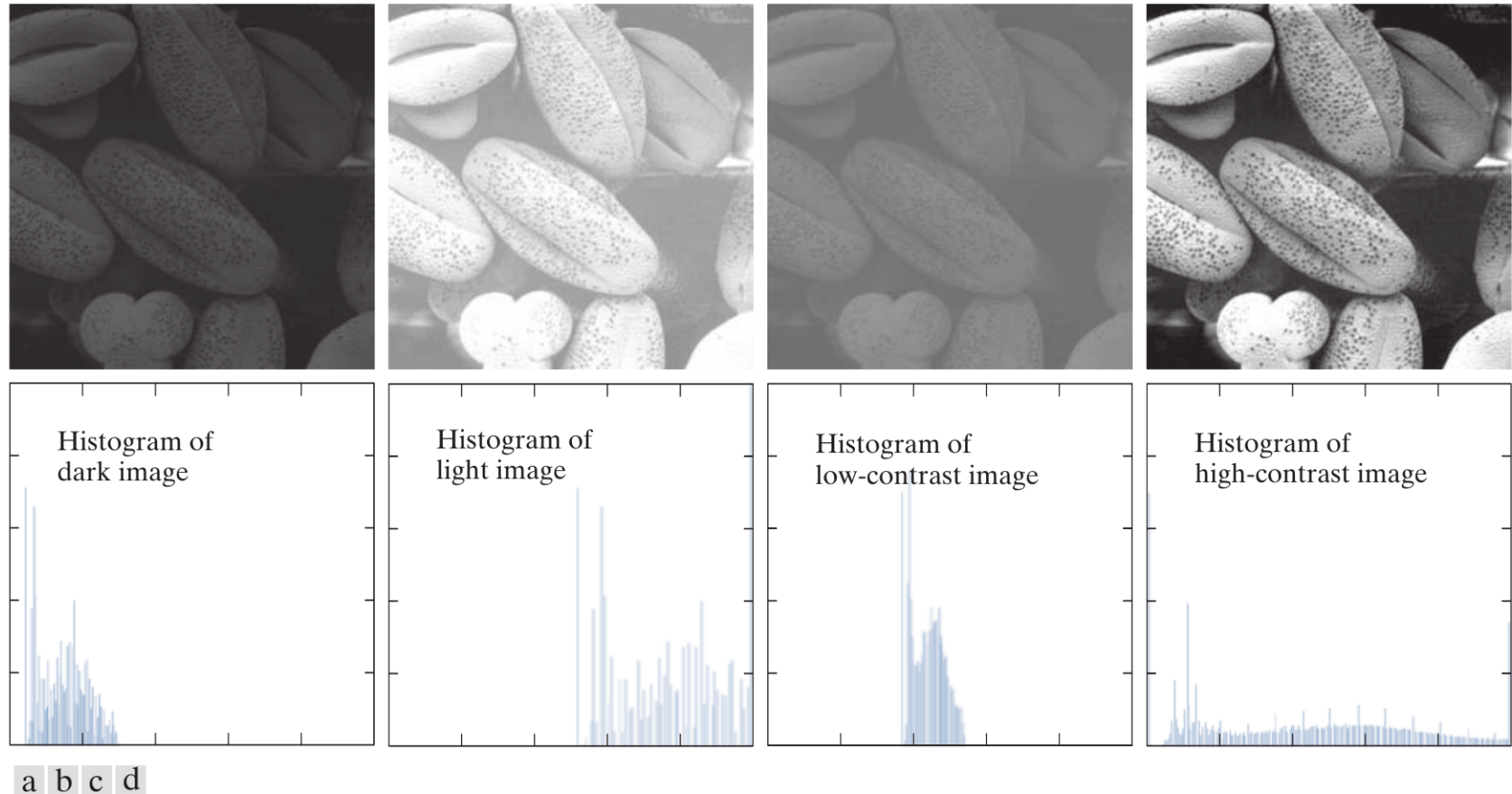


FIGURE 3.16 Four image types and their corresponding histograms. (a) dark; (b) light; (c) low contrast; (d) high contrast. The horizontal axis of the histograms are values of r_k and the vertical axis are values of $p(r_k)$.

直方图均衡

$$s = g(r)$$

$$p(s)ds = p(r)dr$$

$$\frac{1}{L}ds = p(r)dr$$

$$\frac{ds}{dr} = Lp(r)$$

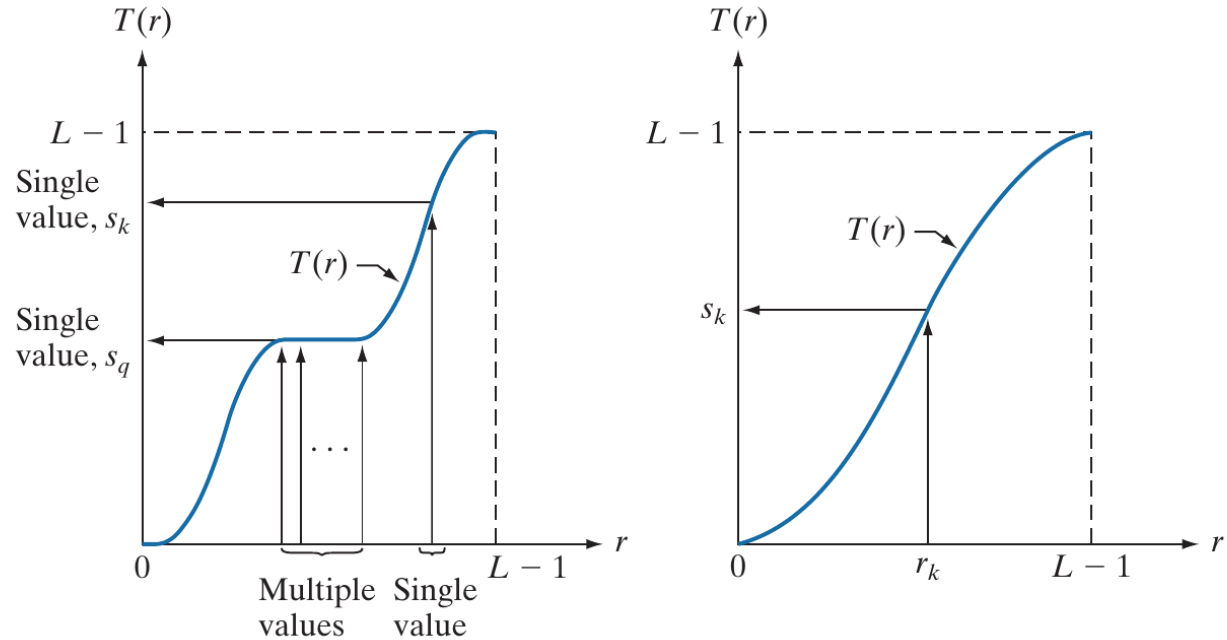
$$s = L \int_0^r p(x)dx$$

单增函数

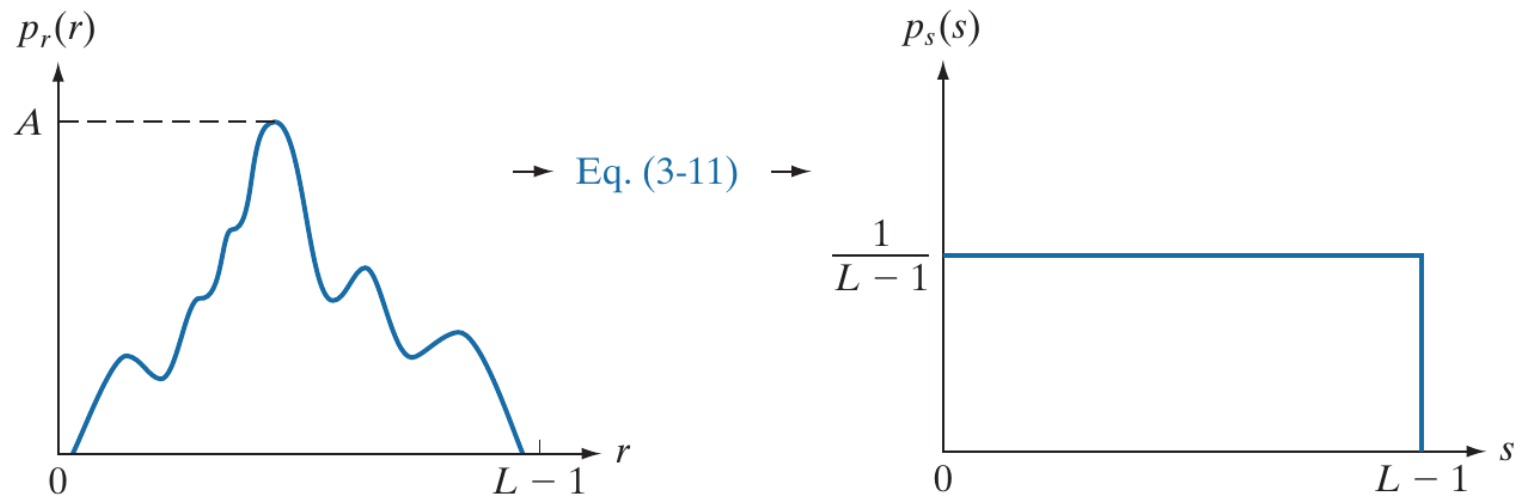
a | b

FIGURE 3.17

(a) Monotonic increasing function, showing how multiple values can map to a single value. (b) Strictly monotonic increasing function. This is a one-to-one mapping, both ways.



概率分布变换



a b

FIGURE 3.18 (a) An arbitrary PDF. (b) Result of applying Eq. (3-11) to the input PDF. The resulting PDF is always uniform, independently of the shape of the input.

直方图变换示例

TABLE 3.1

Intensity distribution and histogram values for a 3-bit, 64×64 digital image.

r_k	n_k	$p_r(r_k) = n_k / MN$
$r_0 = 0$	790	0.19
$r_1 = 1$	1023	0.25
$r_2 = 2$	850	0.21
$r_3 = 3$	656	0.16
$r_4 = 4$	329	0.08
$r_5 = 5$	245	0.06
$r_6 = 6$	122	0.03
$r_7 = 7$	81	0.02

直方图变换示例 (续)

a | b | c

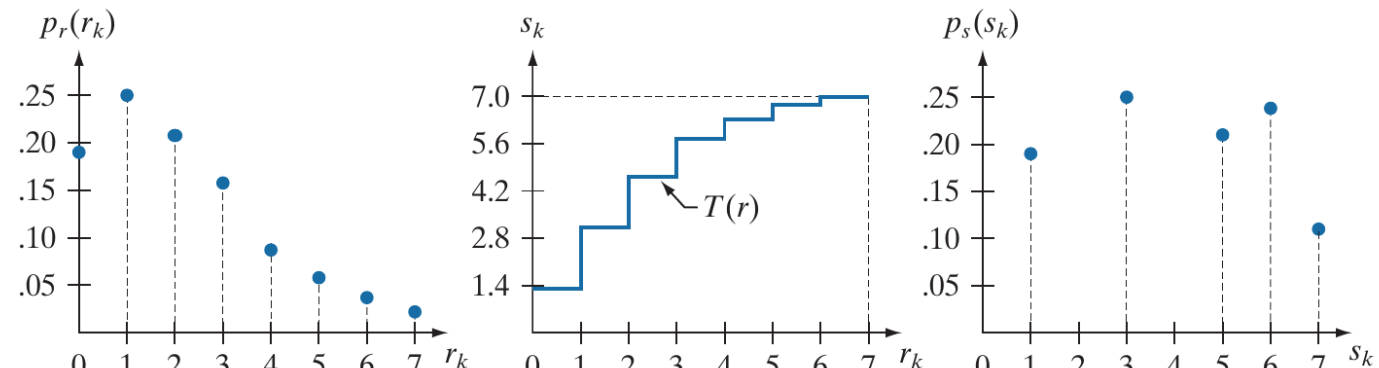
FIGURE 3.19

Histogram equalization.

(a) Original histogram.

(b) Transformation function.

(c) Equalized histogram.



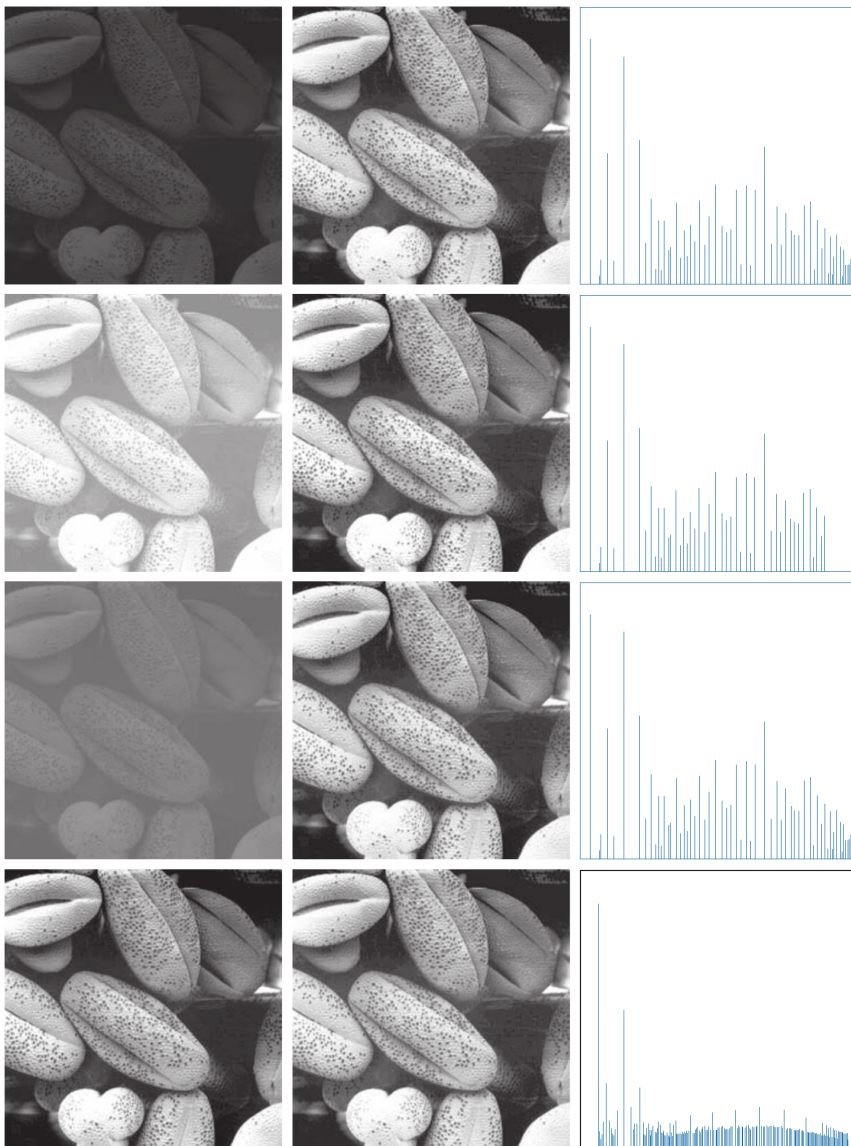
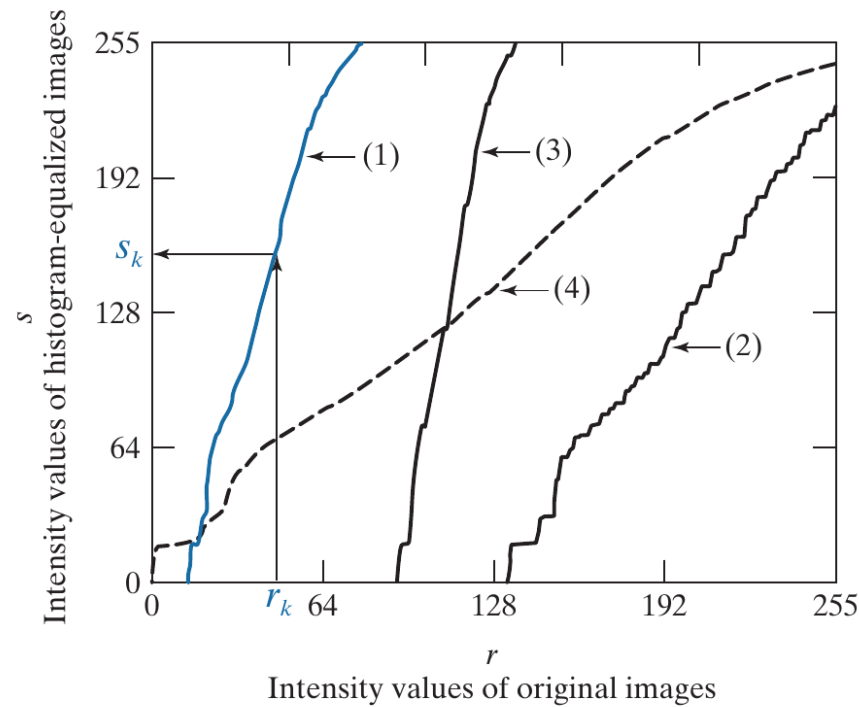


FIGURE 3.20 Left column: Images from Fig. 3.16. Center column: Corresponding histogram-equalized images. Right column: histograms of the images in the center column (compare with the histograms in Fig. 3.16).

^ . ^

FIGURE 3.21

Transformation functions for histogram equalization. Transformations (1) through (4) were obtained using Eq. (3-15) and the histograms of the images on the left column of Fig. 3.20. Mapping of one intensity value r_k in image 1 to its corresponding value s_k is shown.



直方图匹配（规范化）

26/64

$$z = g(s)$$

$$s = g^{-1}(z)$$

$$p(z)dz = p(s)ds$$

$$p(z)dz = \frac{1}{L}ds$$

$$\frac{ds}{dz} = Lp(z)$$

$$s = L \int_0^z p(x)dx$$

^ . ^

a	b
c	d

FIGURE 3.22

- (a) Histogram of a 3-bit image.
 - (b) Specified histogram.
 - (c) Transformation function obtained from the specified histogram.
 - (d) Result of histogram specification. Compare the histograms in (b) and (d).
-

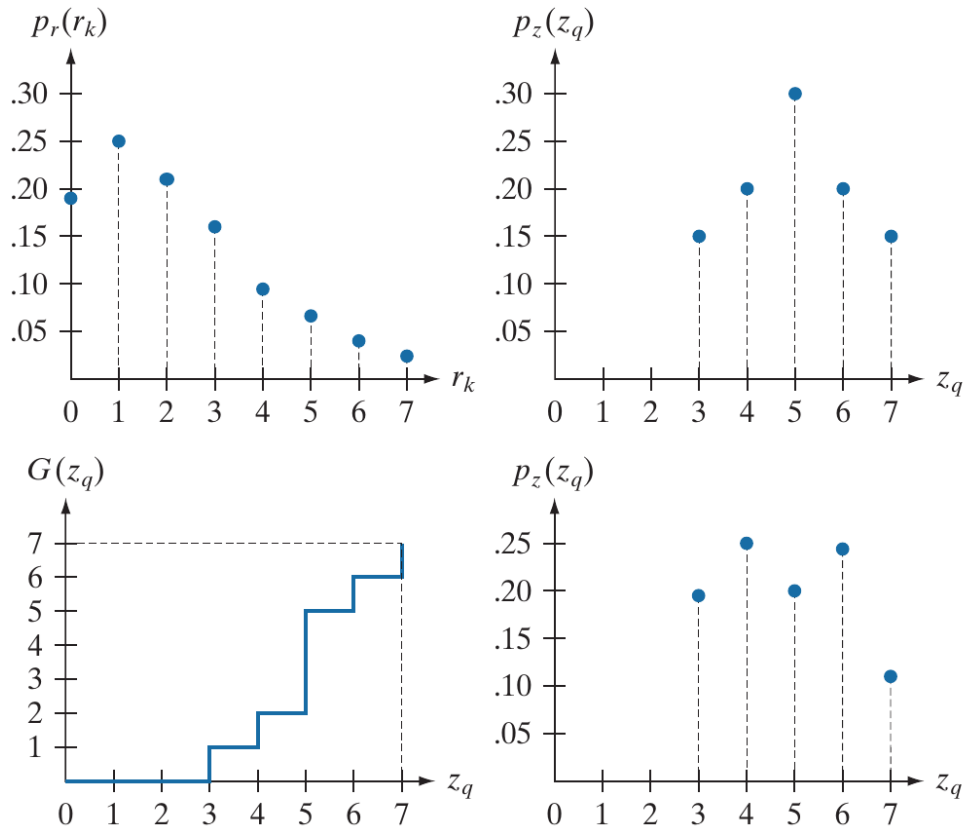


TABLE 3.2

Specified and actual histograms (the values in the third column are computed in Example 3.7).

z_q	Specified $p_z(z_q)$	Actual $p_z(z_q)$
$z_0 = 0$	0.00	0.00
$z_1 = 1$	0.00	0.00
$z_2 = 2$	0.00	0.00
$z_3 = 3$	0.15	0.19
$z_4 = 4$	0.20	0.25
$z_5 = 5$	0.30	0.21
$z_6 = 6$	0.20	0.24
$z_7 = 7$	0.15	0.11

TABLE 3.2

Specified and actual histograms
(the values in
the third column
are computed in
Example 3.7).

z_q	Specified $p_z(z_q)$	Actual $p_z(z_q)$
$z_0 = 0$	0.00	0.00
$z_1 = 1$	0.00	0.00
$z_2 = 2$	0.00	0.00
$z_3 = 3$	0.15	0.19
$z_4 = 4$	0.20	0.25
$z_5 = 5$	0.30	0.21
$z_6 = 6$	0.20	0.24
$z_7 = 7$	0.15	0.11

TABLE 3.3

Rounded values
of the
transformation
function $G(z_q)$.

z_q	$G(z_q)$
$z_0 = 0$	0
$z_1 = 1$	0
$z_2 = 2$	0
$z_3 = 3$	1
$z_4 = 4$	2
$z_5 = 5$	5
$z_6 = 6$	6
$z_7 = 7$	7

TABLE 3.4

Mapping of
values s_k into
corresponding
values z_q .

s_k	\rightarrow	z_q
1	\rightarrow	3
3	\rightarrow	4
5	\rightarrow	5
6	\rightarrow	6
7	\rightarrow	7

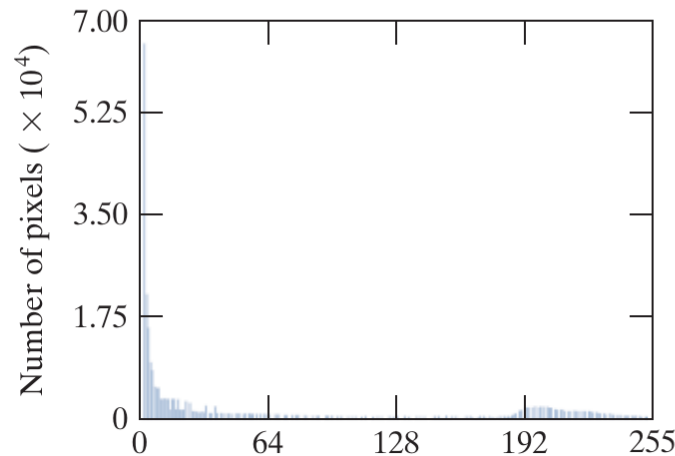
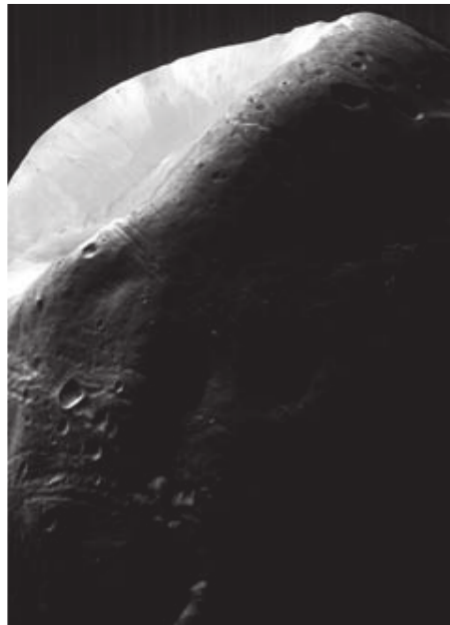
直方图规定化示例

29/64

a | b

FIGURE 3.23

(a) An image, and
(b) its histogram.

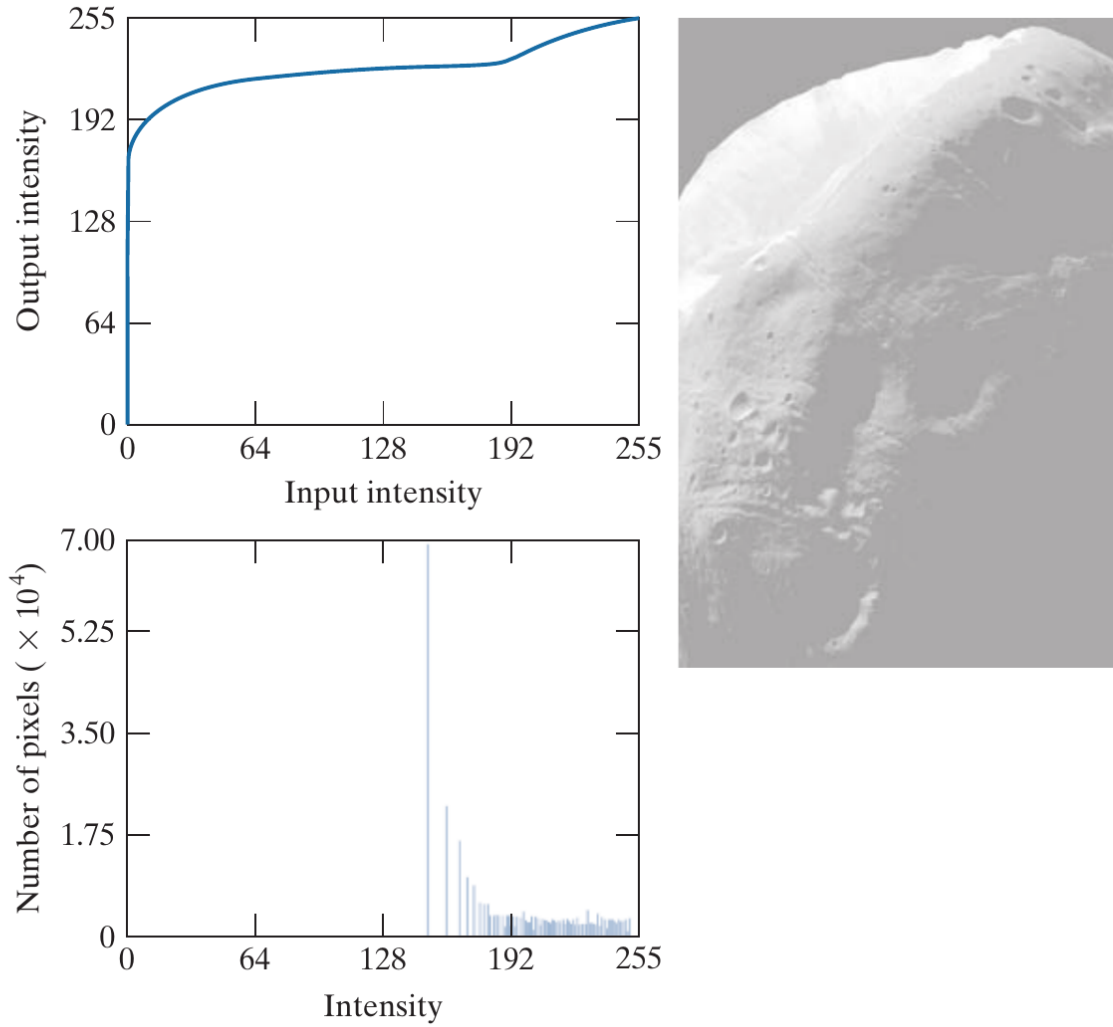


直方图规范化示例（续）

a
b
c

FIGURE 3.24

- (a) Histogram equalization transformation obtained using the histogram in Fig. 3.23(b).
(b) Histogram equalized image.
(c) Histogram of equalized image.

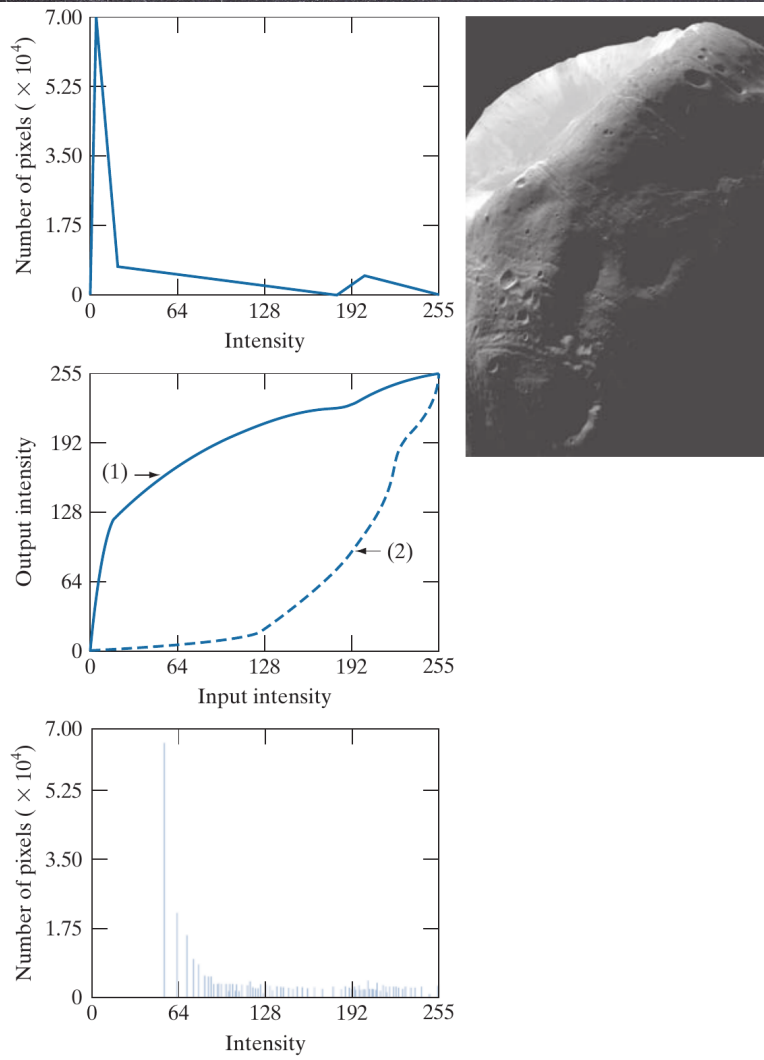


直方图规范化（续）

a
b
c
d

FIGURE 3.25

Histogram specification.
 (a) Specified histogram.
 (b) Transformation $G(z_q)$, labeled (1), and $G^{-1}(s_k)$, labeled (2).
 (c) Result of histogram specification.
 (d) Histogram of image (c).

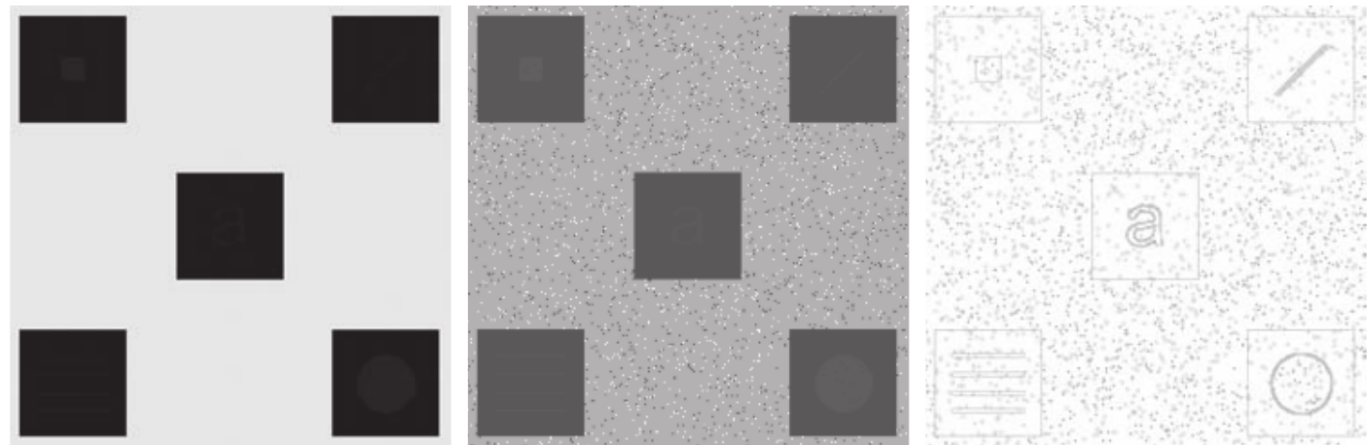


局部直方图均衡

a b c

FIGURE 3.26

- (a) Original image. (b) Result of global histogram equalization.
(c) Result of local histogram equalization.



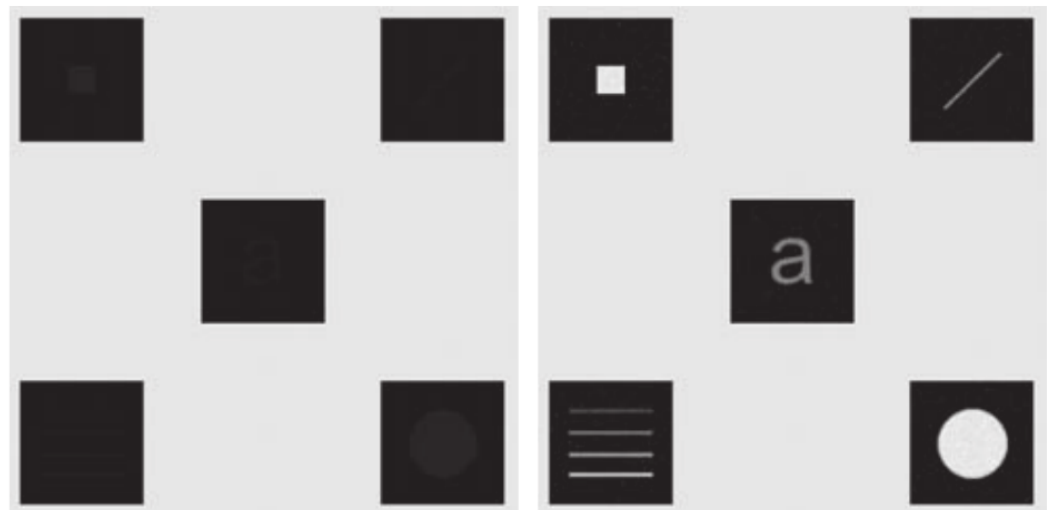
直方图统计图像增强

$$g(x, y) = \begin{cases} Cf(x, y) & k_0 m_G \leq m_{S_{xy}} \leq k_1 m_G, k_2 \sigma_G \leq \sigma_{S_{xy}} \leq k_3 \sigma_G \\ f(x, y) & \text{otherwise} \end{cases}$$

a b

FIGURE 3.27

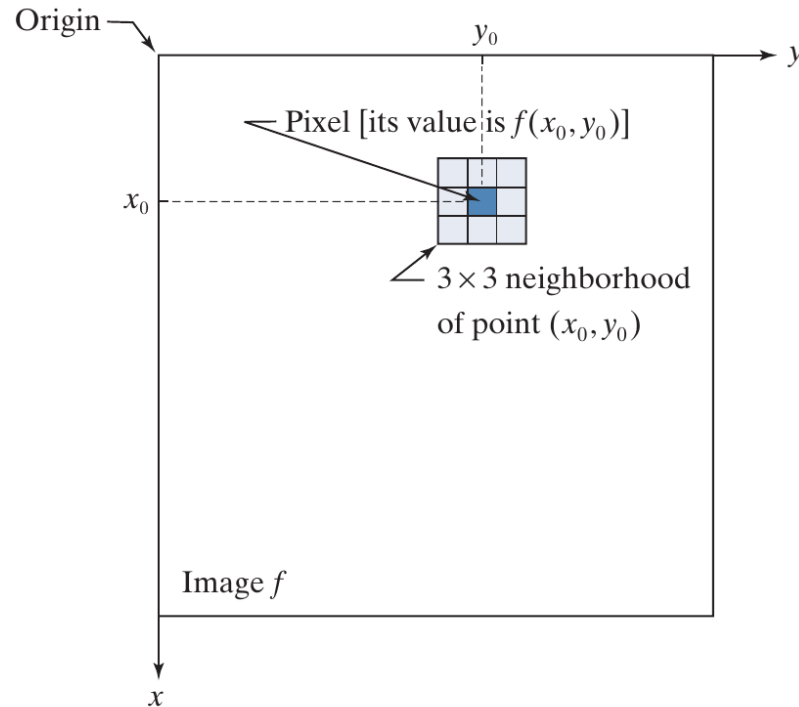
(a) Original image. (b) Result of local enhancement based on local histogram statistics.
Compare (b) with Fig. 3.26(c).



邻域

FIGURE 3.1

A 3×3 neighborhood about a point (x_0, y_0) in an image. The neighborhood is moved from pixel to pixel in the image to generate an output image. Recall from Chapter 2 that the value of a pixel at location (x_0, y_0) is $f(x_0, y_0)$, the value of the image at that location.

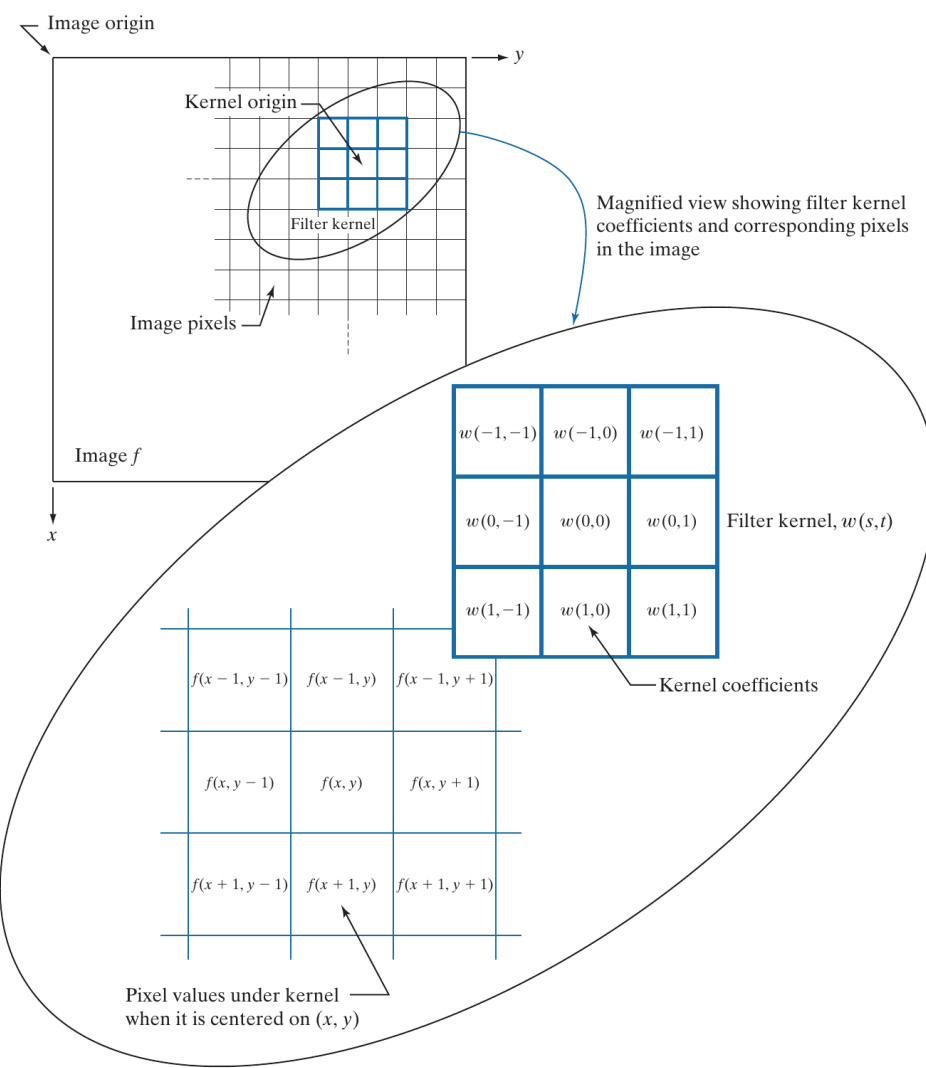


空间相关与卷积

35/64

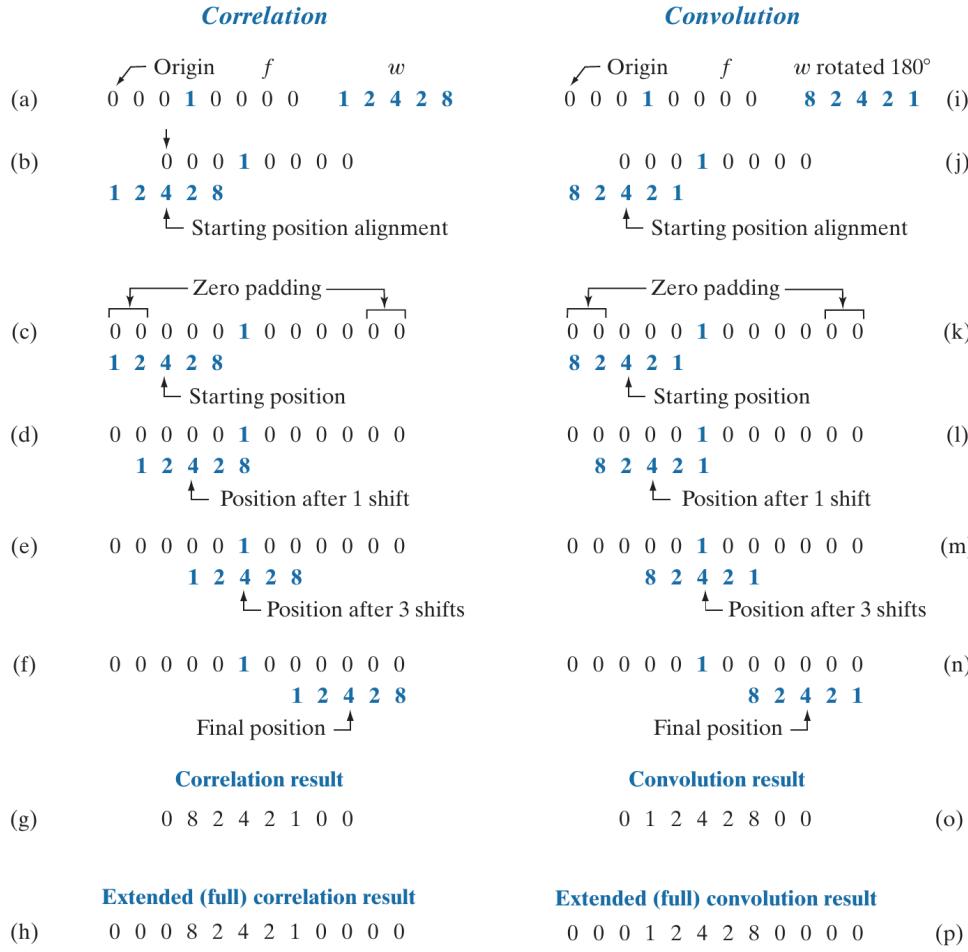
FIGURE 3.28

The mechanics of linear spatial filtering using a 3×3 kernel. The pixels are shown as squares to simplify the graphics. Note that the origin of the image is at the top left, but the origin of the kernel is at its center. Placing the origin at the center of spatially symmetric kernels simplifies writing expressions for linear filtering.



相关与卷积

FIGURE 3.29
 Illustration of 1-D correlation and convolution of a kernel, w , with a function f consisting of a discrete unit impulse. Note that correlation and convolution are functions of the variable x , which acts to *displace* one function with respect to the other. For the extended correlation and convolution results, the starting configuration places the right-most element of the kernel to be coincident with the origin of f . Additional padding must be used.



2-D相关与卷积

FIGURE 3.30

Correlation (middle row) and convolution (last row) of a 2-D kernel with an image consisting of a discrete unit impulse. The 0's are shown in gray to simplify visual analysis. Note that correlation and convolution are functions of x and y . As these variable change, they displace one function with respect to the other. See the discussion of Eqs. (3-36) and (3-37) regarding full correlation and convolution.

		Padded f					
\nwarrow Origin f		0	0	0	0	0	0
0	0	0	0	0	0	0	0
0	0	0	0	0	0	0	0
0	0	0	0	0	0	0	0
w		0	0	0	1	0	0
0	0	1	0	0	1	2	3
0	0	0	0	0	4	5	6
0	0	0	0	0	7	8	9
(a)		(b)					
\nwarrow Initial position for w		Correlation result			Full correlation result		
1	2	3	0	0	0	0	0
4	5	6	0	0	0	0	0
7	8	9	0	0	0	0	0
0	0	0	1	0	0	0	0
0	0	0	0	0	0	6	5
0	0	0	0	0	0	3	2
0	0	0	0	0	0	0	0
0	0	0	0	0	0	0	0
(c)		(d)			(e)		
\nwarrow Rotated w		Convolution result			Full convolution result		
9	8	7	0	0	0	0	0
6	5	4	0	0	0	0	0
3	2	1	0	0	0	1	2
0	0	0	1	0	0	4	5
0	0	0	0	0	0	7	8
0	0	0	0	0	0	0	0
0	0	0	0	0	0	0	0
(f)		(g)			(h)		

平滑核示例

a | b

FIGURE 3.31

Examples of smoothing kernels:
(a) is a *box* kernel;
(b) is a *Gaussian* kernel.

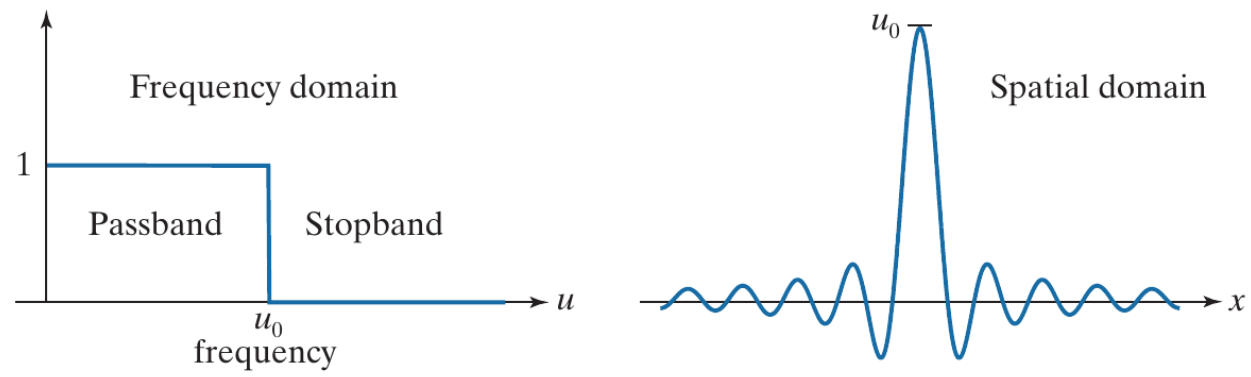
$$\frac{1}{9} \times \begin{array}{|c|c|c|} \hline 1 & 1 & 1 \\ \hline 1 & 1 & 1 \\ \hline 1 & 1 & 1 \\ \hline \end{array} \quad \frac{1}{4.8976} \times \begin{array}{|c|c|c|} \hline 0.3679 & 0.6065 & 0.3679 \\ \hline 0.6065 & 1.0000 & 0.6065 \\ \hline 0.3679 & 0.6065 & 0.3679 \\ \hline \end{array}$$

空间域与频域低通滤波

a | b

FIGURE 3.32

- (a) Ideal 1-D low-pass filter transfer function in the frequency domain.
(b) Corresponding filter kernel in the spatial domain.



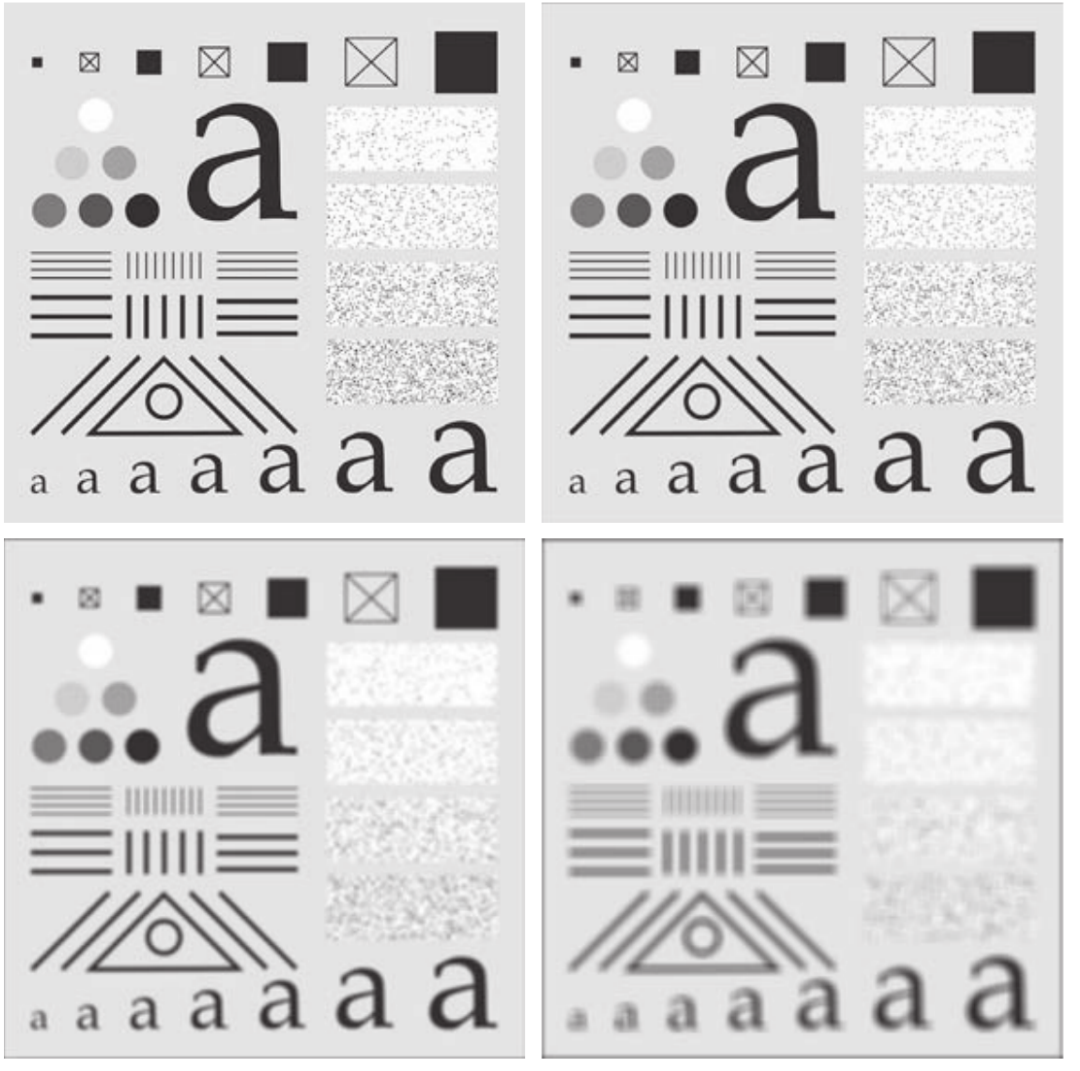
Box kernel

a b
c d

FIGURE 3.33

(a) Test pattern of size 1024×1024 pixels.

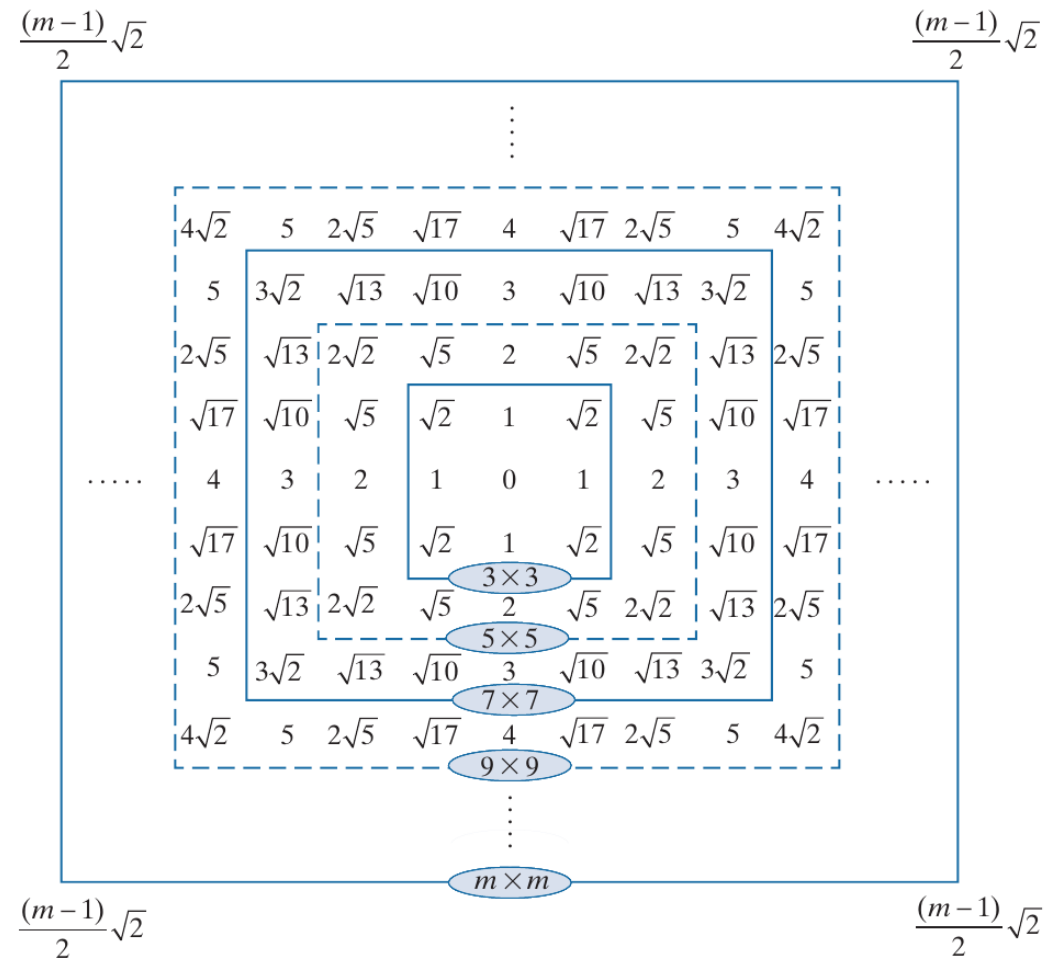
(b)-(d) Results of lowpass filtering with box kernels of sizes 3×3 , 11×11 , and 21×21 , respectively.



距离

FIGURE 3.34

Distances from the center for various sizes of square kernels.

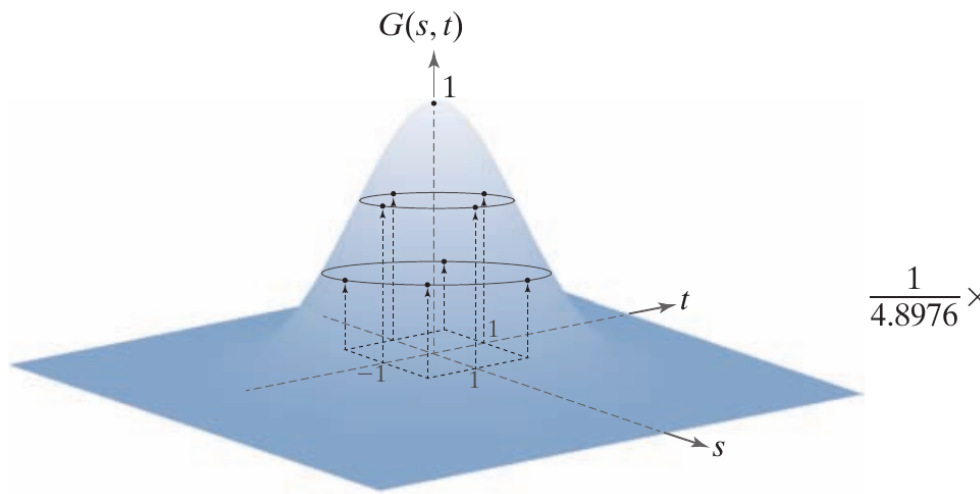


高斯核

a b

FIGURE 3.35

(a) Sampling a Gaussian function to obtain a discrete Gaussian kernel. The values shown are for $K = 1$ and $\sigma = 1$. (b) Resulting 3×3 kernel [this is the same as Fig. 3.31(b)].



$$\frac{1}{4.8976} \times$$

0.3679	0.6065	0.3679
0.6065	1.0000	0.6065
0.3679	0.6065	0.3679

高斯核濾波

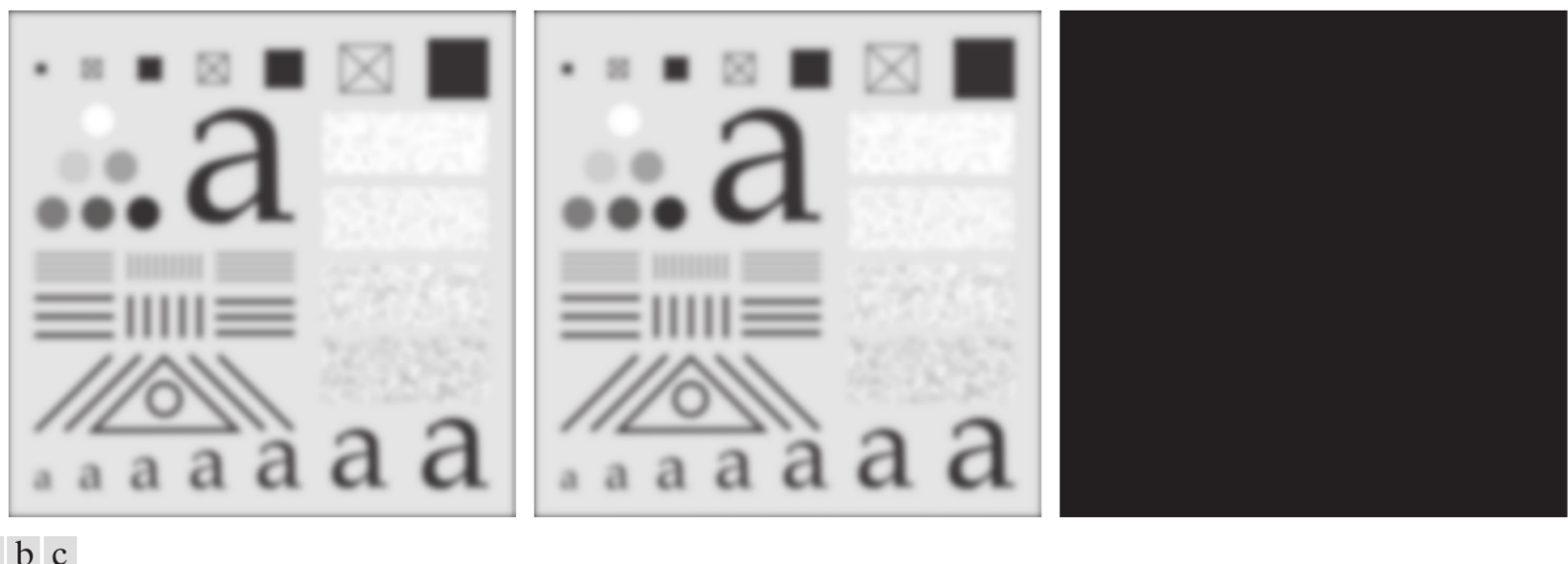
43/64



a b c

FIGURE 3.36 (a) A test pattern of size 1024×1024 . (b) Result of lowpass filtering the pattern with a Gaussian kernel of size 21×21 , with standard deviations $\sigma = 3.5$. (c) Result of using a kernel of size 43×43 , with $\sigma = 7$. This result is comparable to Fig. 3.33(d). We used $K = 1$ in all cases.

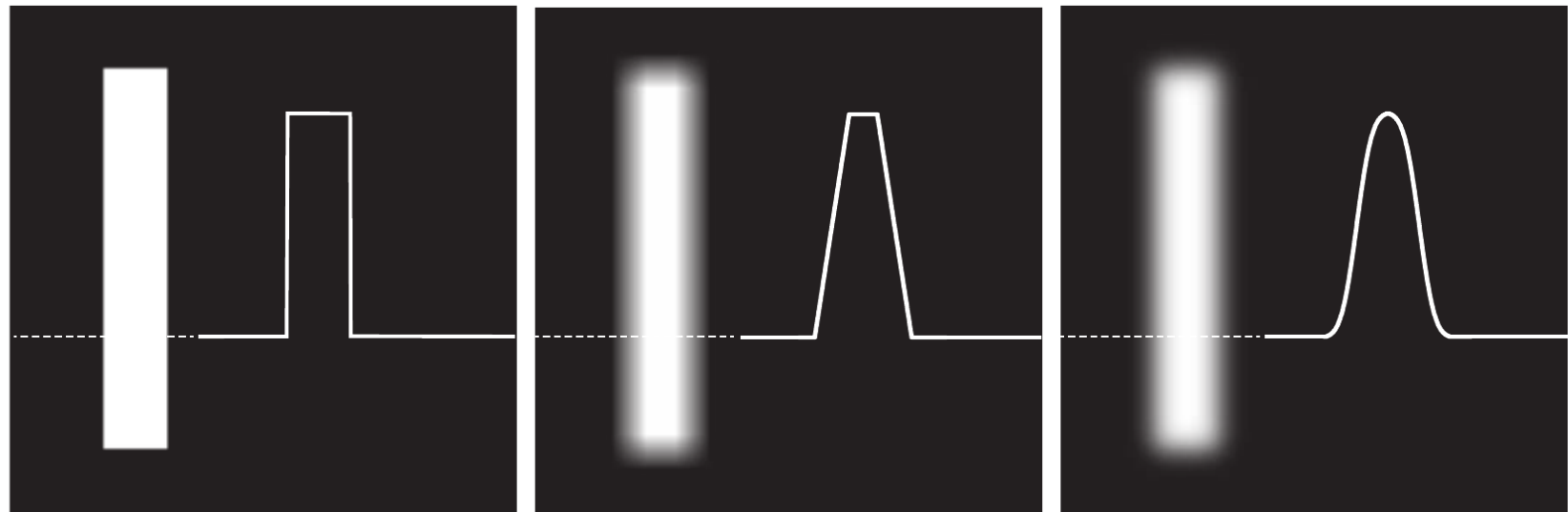
不同尺度高斯濾波



a b c

FIGURE 3.37 (a) Result of filtering Fig. 3.36(a) using a Gaussian kernels of size 43×43 , with $\sigma = 7$. (b) Result of using a kernel of 85×85 , with the same value of σ . (c) Difference image.

平滑效果比较

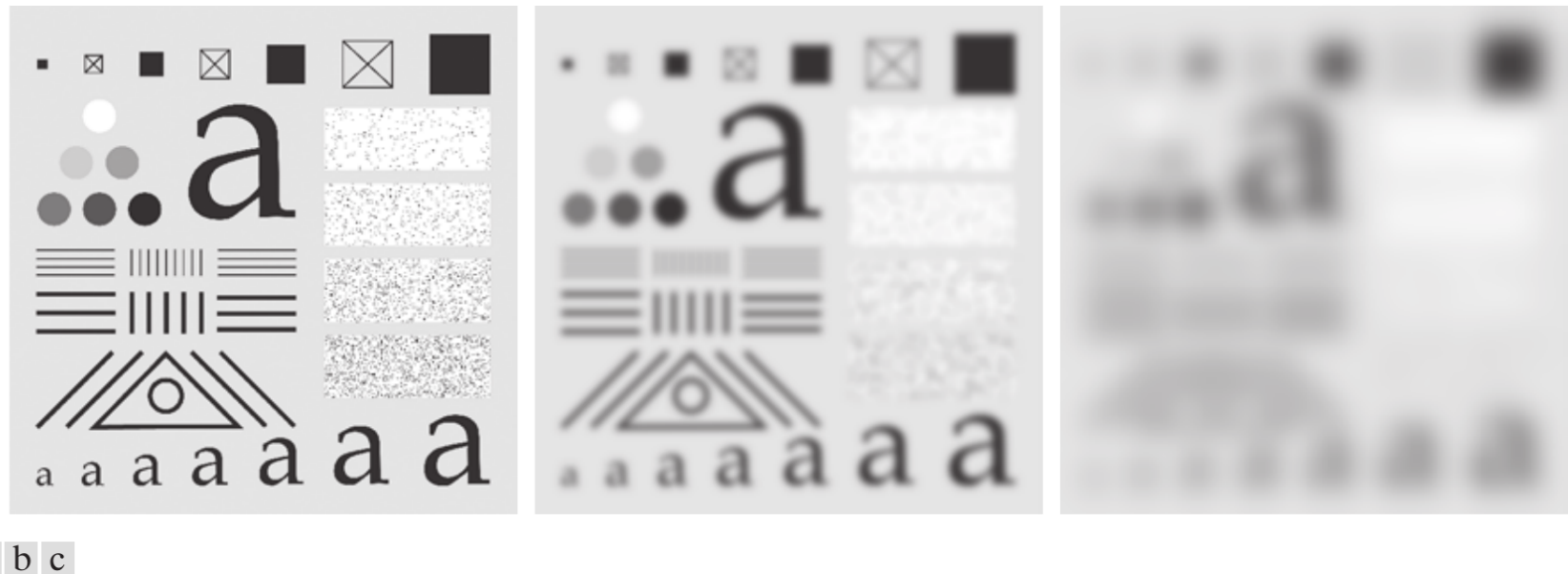


a b c

FIGURE 3.38 (a) Image of a white rectangle on a black background, and a horizontal intensity profile along the scan line shown dotted. (b) Result of smoothing this image with a box kernel of size 71×71 , and corresponding intensity profile. (c) Result of smoothing the image using a Gaussian kernel of size 151×151 , with $K = 1$ and $\sigma = 25$. Note the smoothness of the profile in (c) compared to (b). The image and rectangle are of sizes 1024×1024 and 768×128 pixels, respectively.

图像大小的影响

46/64



a b c

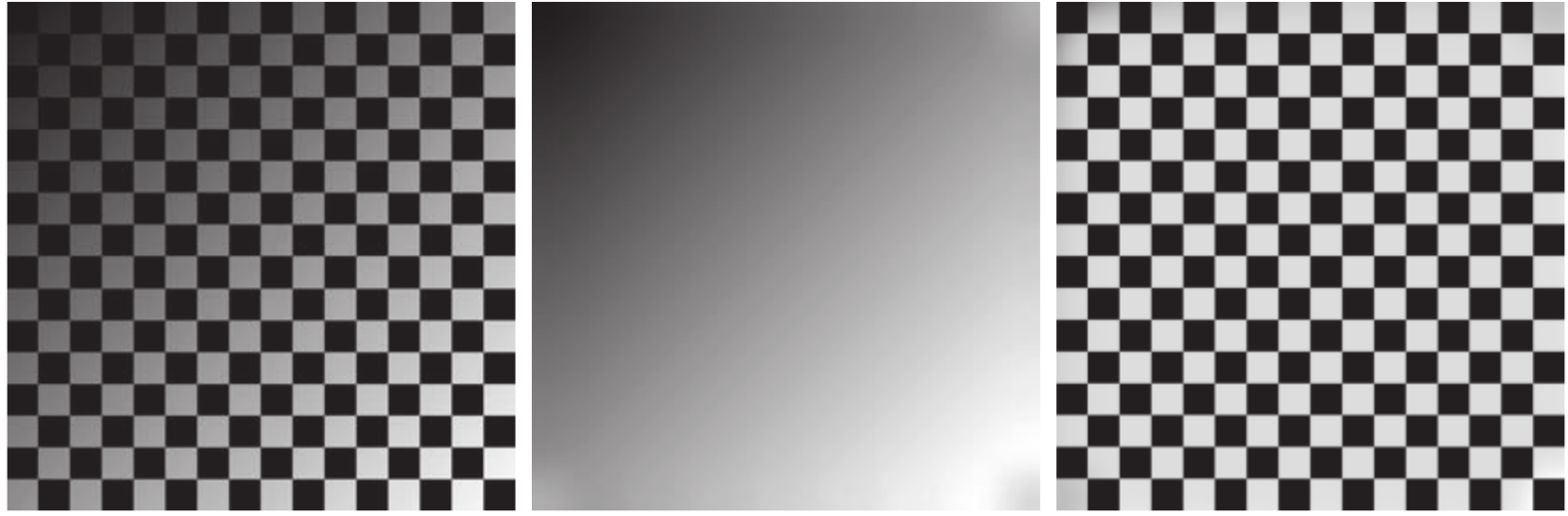
FIGURE 3.40 (a) Test pattern of size 4096×4096 pixels. (b) Result of filtering the test pattern with the same Gaussian kernel used in Fig. 3.39. (c) Result of filtering the pattern using a Gaussian kernel of size 745×745 elements, with $K = 1$ and $\sigma = 124$. Mirror padding was used throughout.

低通閾值區域提取



a b c

FIGURE 3.41 (a) A 2566×2758 Hubble Telescope image of the *Hickson Compact Group*. (b) Result of lowpass filtering with a Gaussian kernel. (c) Result of thresholding the filtered image (intensities were scaled to the range $[0, 1]$). The Hickson Compact Group contains dwarf galaxies that have come together, setting off thousands of new star clusters. (Original image courtesy of NASA.)

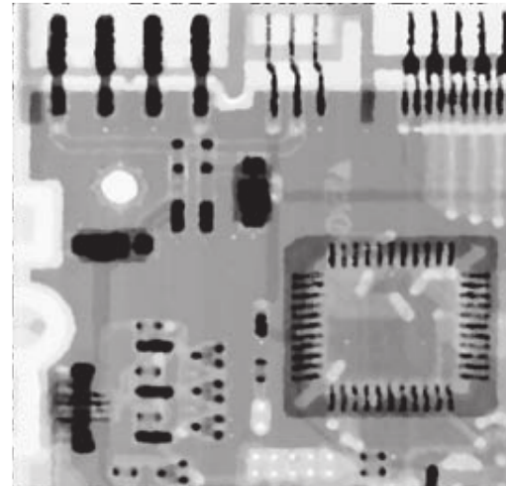
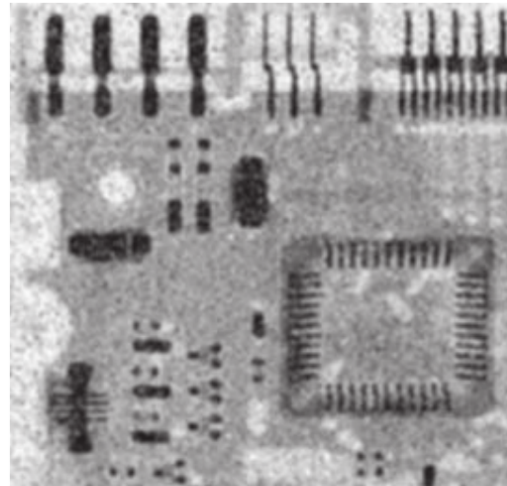
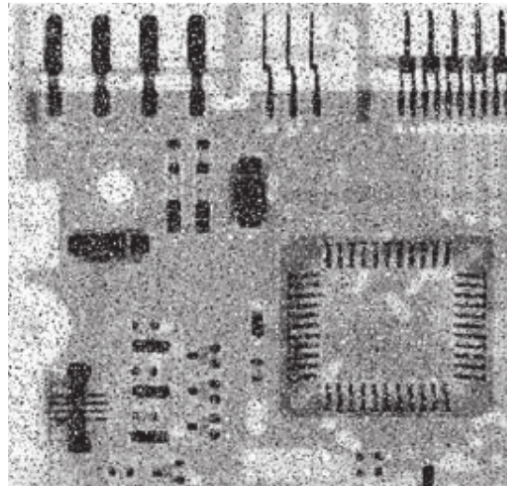


a b c

FIGURE 3.42 (a) Image shaded by a shading pattern oriented in the -45° direction. (b) Estimate of the shading patterns obtained using lowpass filtering. (c) Result of dividing (a) by (b). (See Section 9.8 for a morphological approach to shading correction).

次序统计滤波

49/64



a b c

FIGURE 3.43 (a) X-ray image of a circuit board, corrupted by salt-and-pepper noise. (b) Noise reduction using a 19×19 Gaussian lowpass filter kernel with $\sigma = 3$. (c) Noise reduction using a 7×7 median filter. (Original image courtesy of Mr. Joseph E. Pascente, Lixi, Inc.)

一阶与二阶导数

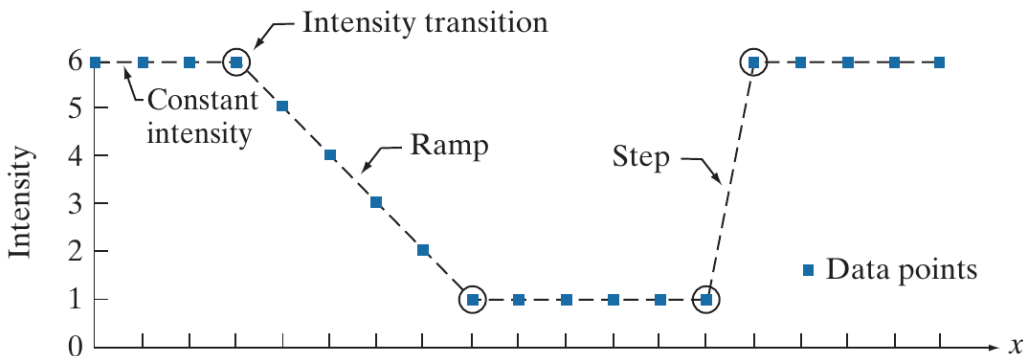
a
b
c

FIGURE 3.44

(a) A section of a horizontal scan line from an image, showing ramp and step edges, as well as constant segments.

(b) Values of the scan line and its derivatives.

(c) Plot of the derivatives, showing a zero crossing. In (a) and (c) points were joined by dashed lines as a visual aid.



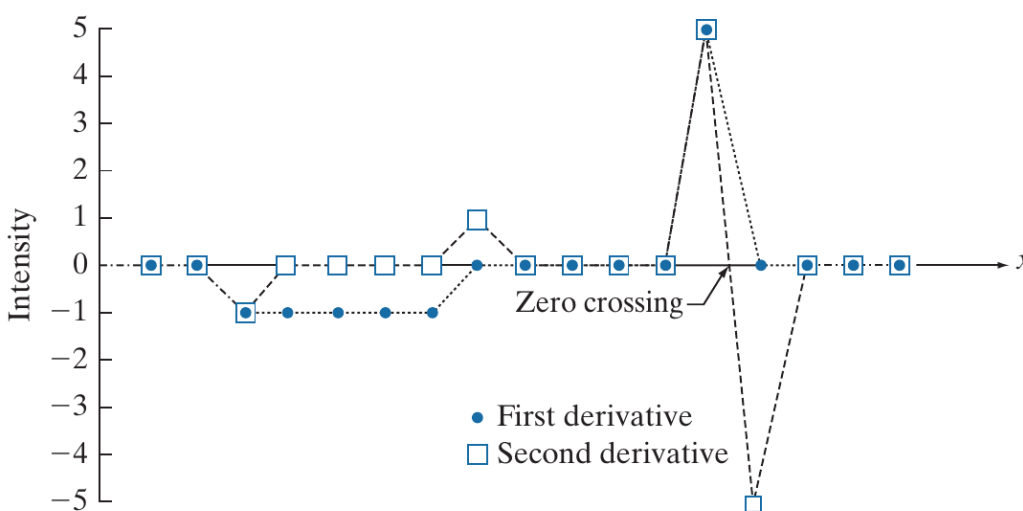
Values of scan line

6	6	6	6	5	4	3	2	1	1	1	1	1	1	6	6	6	6	6

 → x

1st derivative 0 0 -1 -1 -1 -1 0 0 0 0 0 0 5 0 0 0 0 0

2nd derivative 0 0 -1 0 0 0 0 1 0 0 0 0 0 5 -5 0 0 0 0



Laplacian kernel

0	1	0
1	-4	1
0	1	0

1	1	1
1	-8	1
1	1	1

0	-1	0
-1	4	-1
0	-1	0

-1	-1	-1
-1	8	-1
-1	-1	-1

a b c d

FIGURE 3.45 (a) Laplacian kernel used to implement Eq. (3-53). (b) Kernel used to implement an extension of this equation that includes the diagonal terms. (c) and (d) Two other Laplacian kernels.

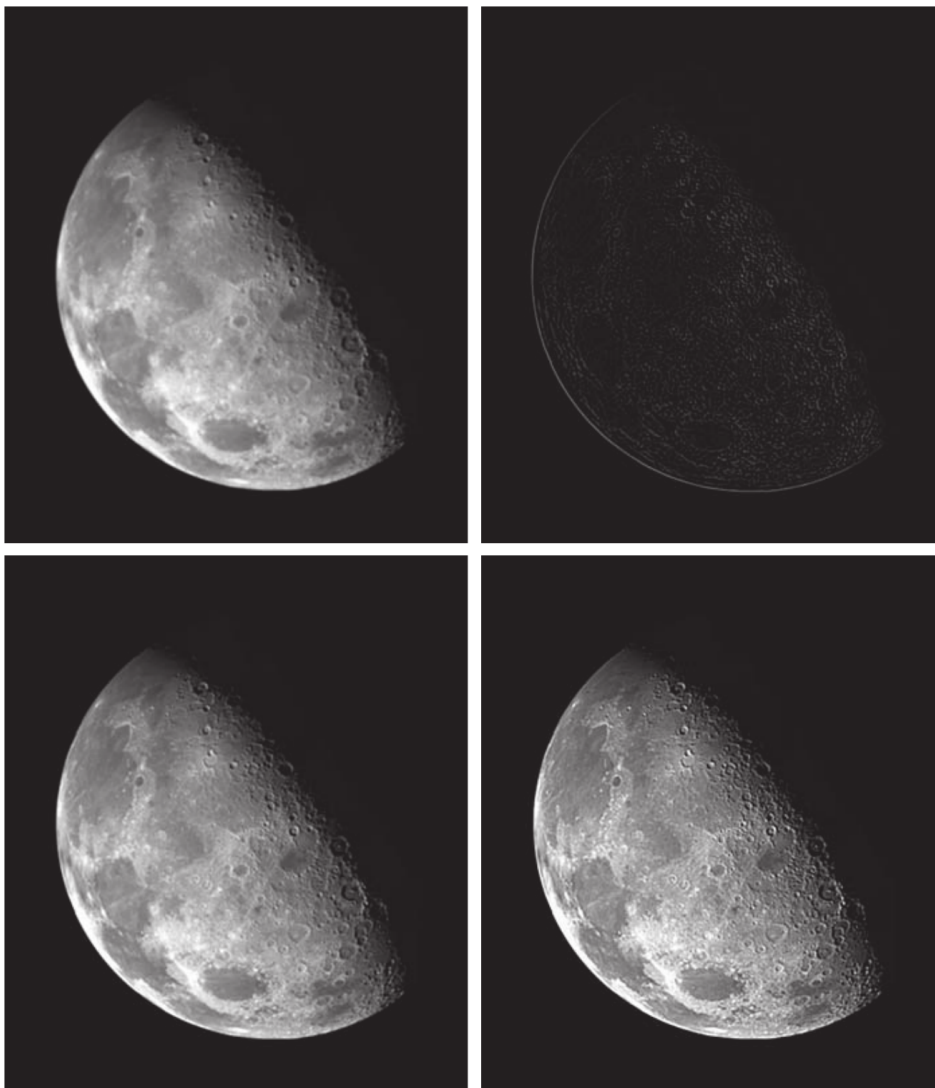
图像锐化示例

52/64

a b
c d

FIGURE 3.46

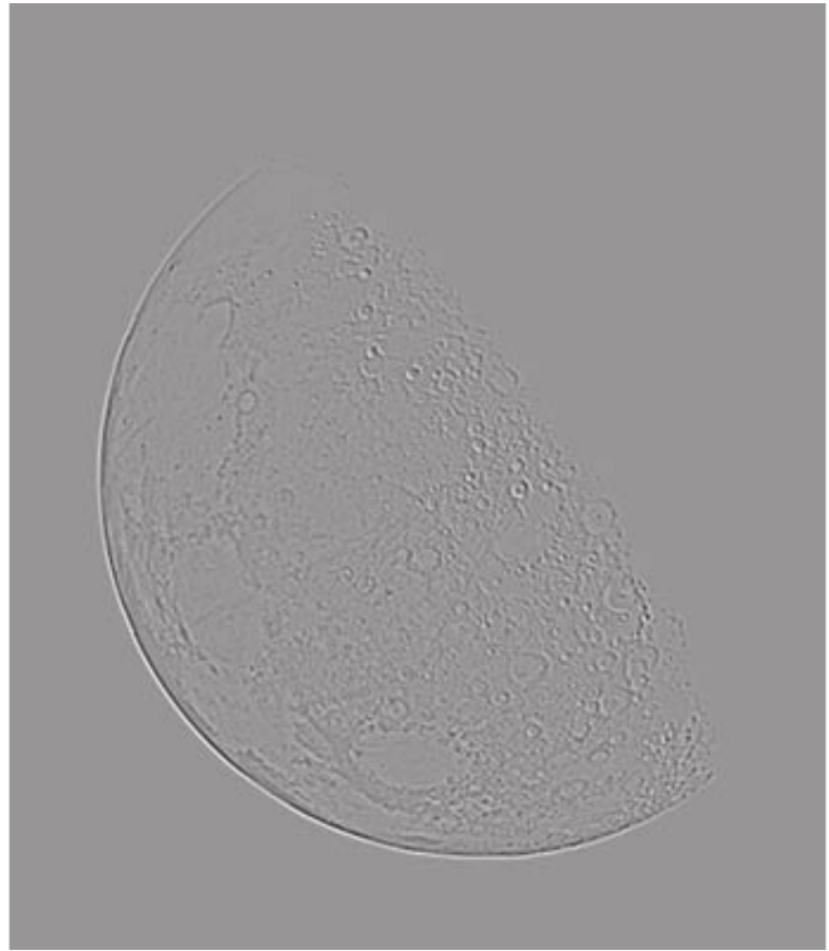
- (a) Blurred image of the North Pole of the moon.
(b) Laplacian image obtained using the kernel in Fig. 3.45(a).
(c) Image sharpened using Eq. (3-54) with $c = -1$.
(d) Image sharpened using the same procedure, but with the kernel in Fig. 3.45(b).
(Original image courtesy of NASA.)
-



图像锐化示例（续）

FIGURE 3.47

The Laplacian image from Fig. 3.46(b), scaled to the full [0, 255] range of intensity values. Black pixels correspond to the most negative value in the unscaled Laplacian image, grays are intermediate values, and white pixels corresponds to the highest positive value.



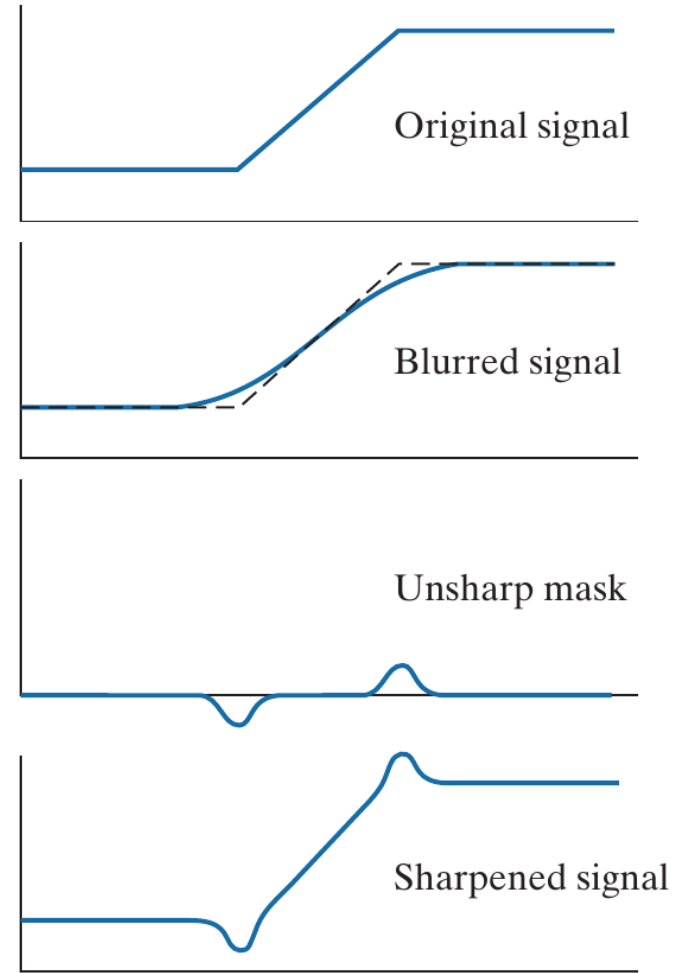
反锐化掩模

a
b
c
d

FIGURE 3.48

1-D illustration of the mechanics of unsharp masking.

- (a) Original signal.
- (b) Blurred signal with original shown dashed for reference.
- (c) Unsharp mask.
- (d) Sharpened signal, obtained by adding (c) to (a).





a	b	c
d	e	

FIGURE 3.49 (a) Original image of size 600×259 pixels. (b) Image blurred using a 31×31 Gaussian lowpass filter with $\sigma = 5$. (c) Mask. (d) Result of unsharp masking using Eq. (3-56) with $k = 1$. (e) Result of highboost filtering with $k = 4.5$.

梯度

a
b
c
d
e

FIGURE 3.50

- (a) A 3×3 region of an image, where the z s are intensity values.
- (b)–(c) Roberts cross-gradient operators.
- (d)–(e) Sobel operators. All the kernel coefficients sum to zero, as expected of a derivative operator.

z_1	z_2	z_3
z_4	z_5	z_6
z_7	z_8	z_9

-1	0
0	1

0	-1
1	0

-1	-2	-1
0	0	0
1	2	1

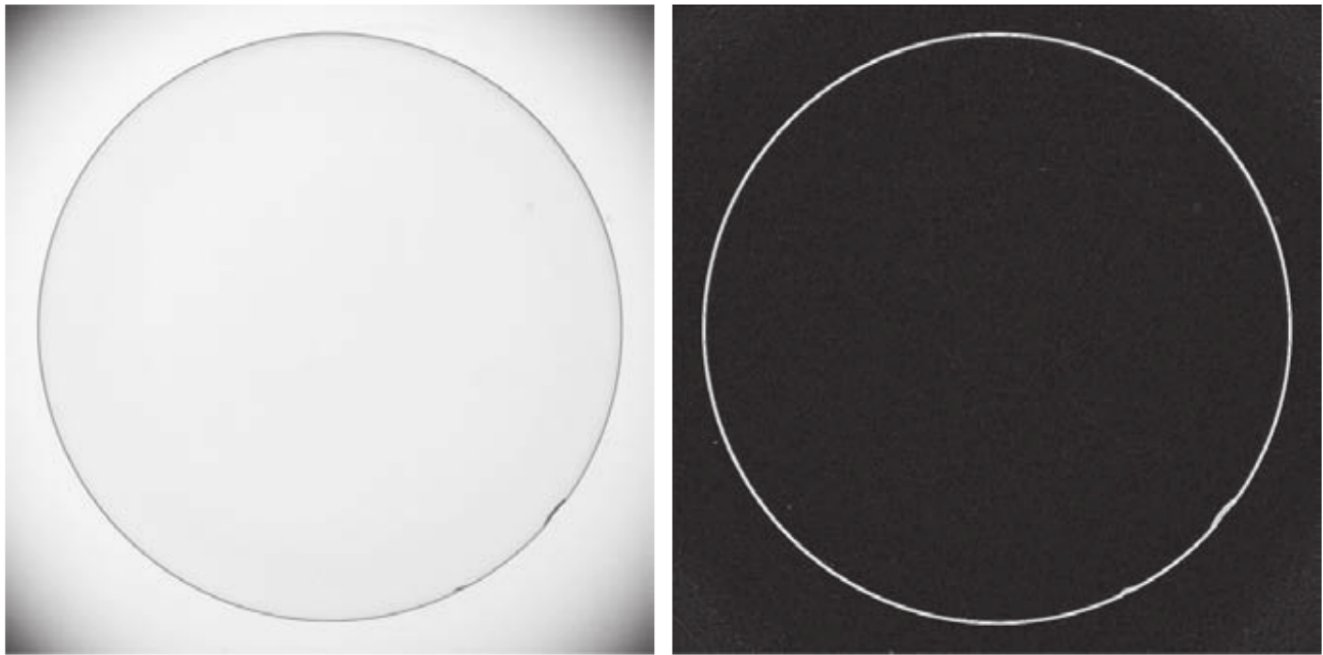
-1	0	1
-2	0	2
-1	0	1

a | b

FIGURE 3.51

(a) Image of a contact lens (note defects on the boundary at 4 and 5 o'clock).

(b) Sobel gradient. (Original image courtesy of Perceptics Corporation.)



高通、带通濾波器

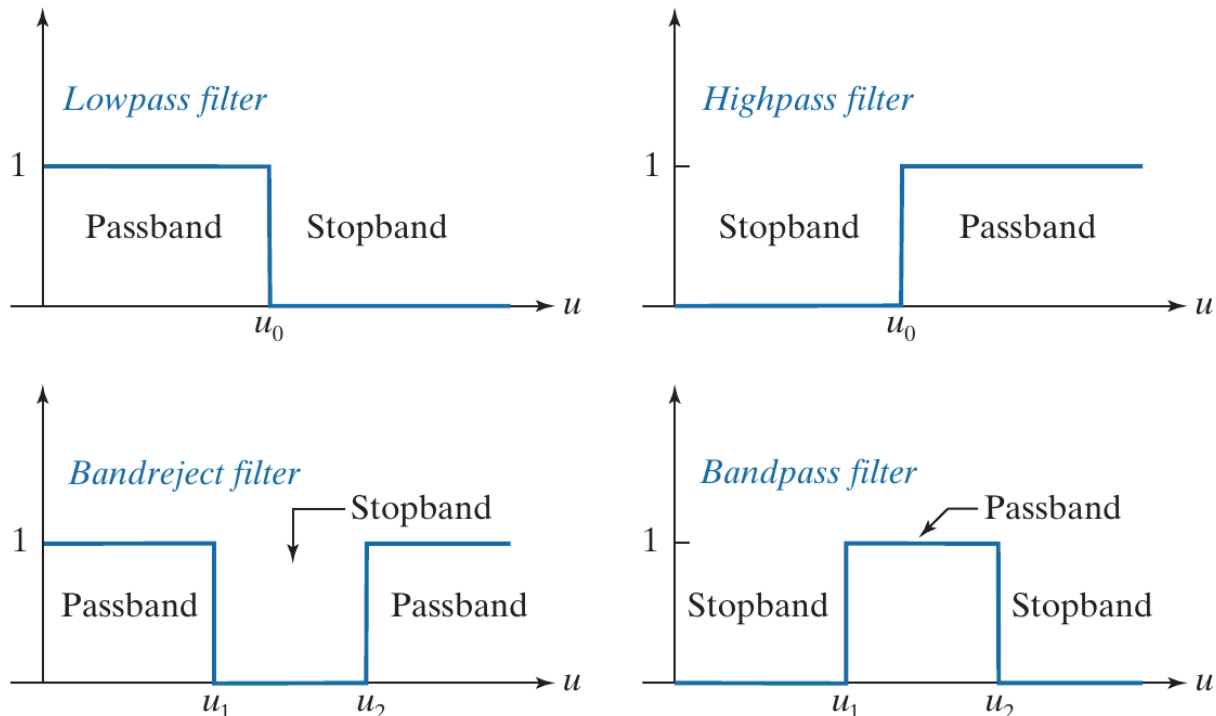
a	b
c	d

FIGURE 3.52

Transfer functions of ideal 1-D filters in the frequency domain (u denotes frequency).

- (a) Lowpass filter.
- (b) Highpass filter.
- (c) Bandreject filter.
- (d) Bandpass filter.

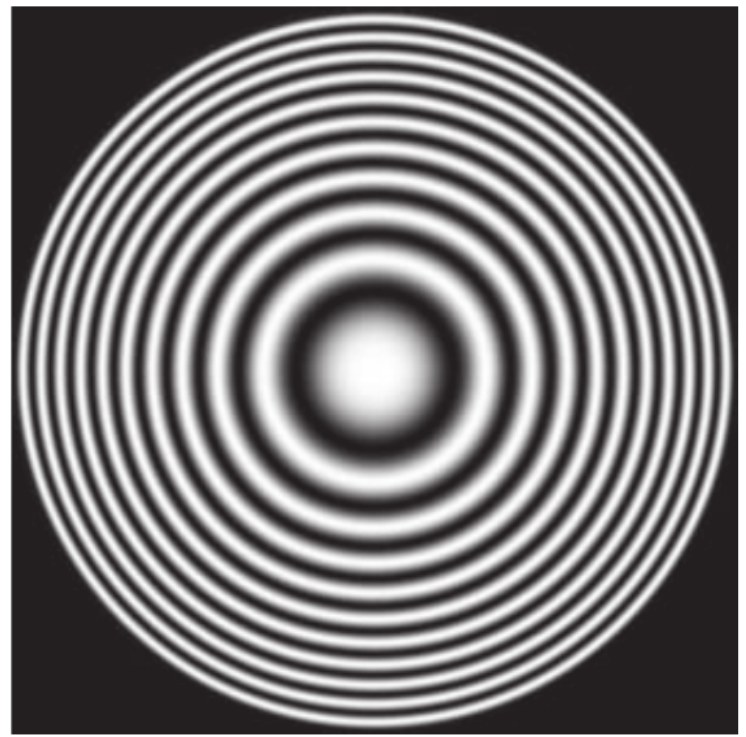
(As before, we show only positive frequencies for simplicity.)



示例图像

FIGURE 3.53

A zone plate
image of size
 597×597 pixels.



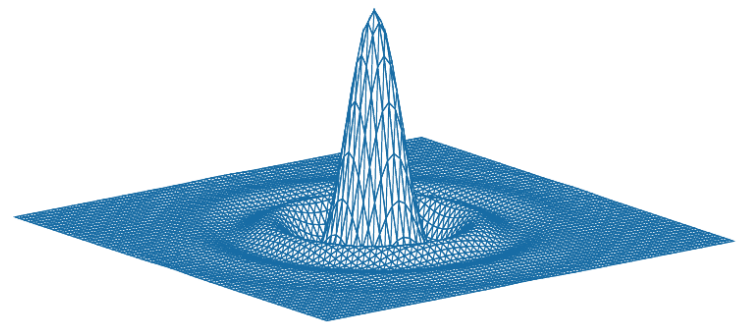
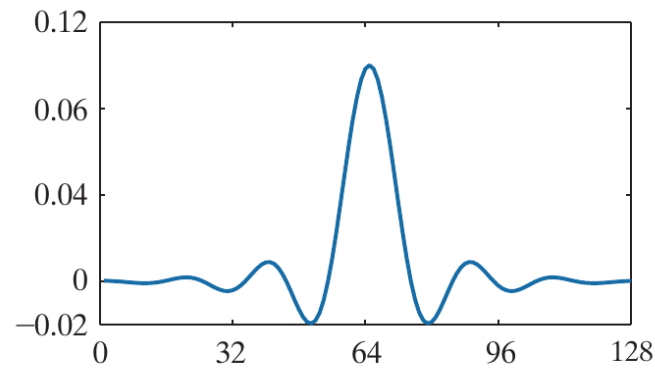
1维与2维滤波器

60/64

a

b

FIGURE 3.54
(a) A 1-D spatial
lowpass filter
function. (b) 2-D
kernel obtained
by rotating the
1-D profile about
its center.



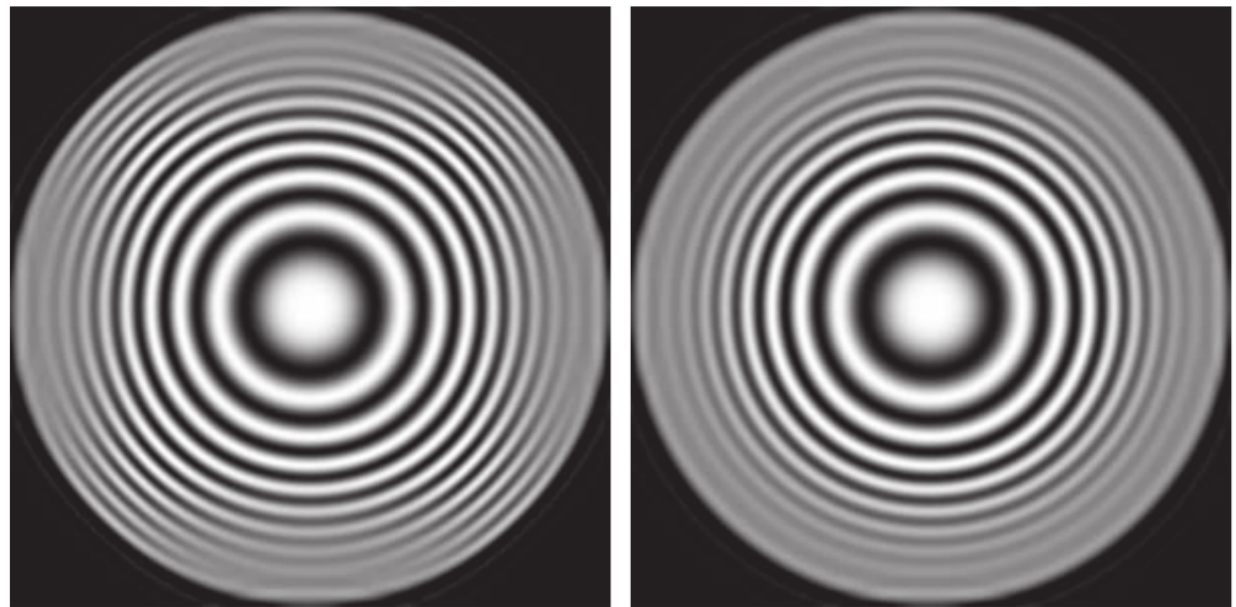
不同濾波效果

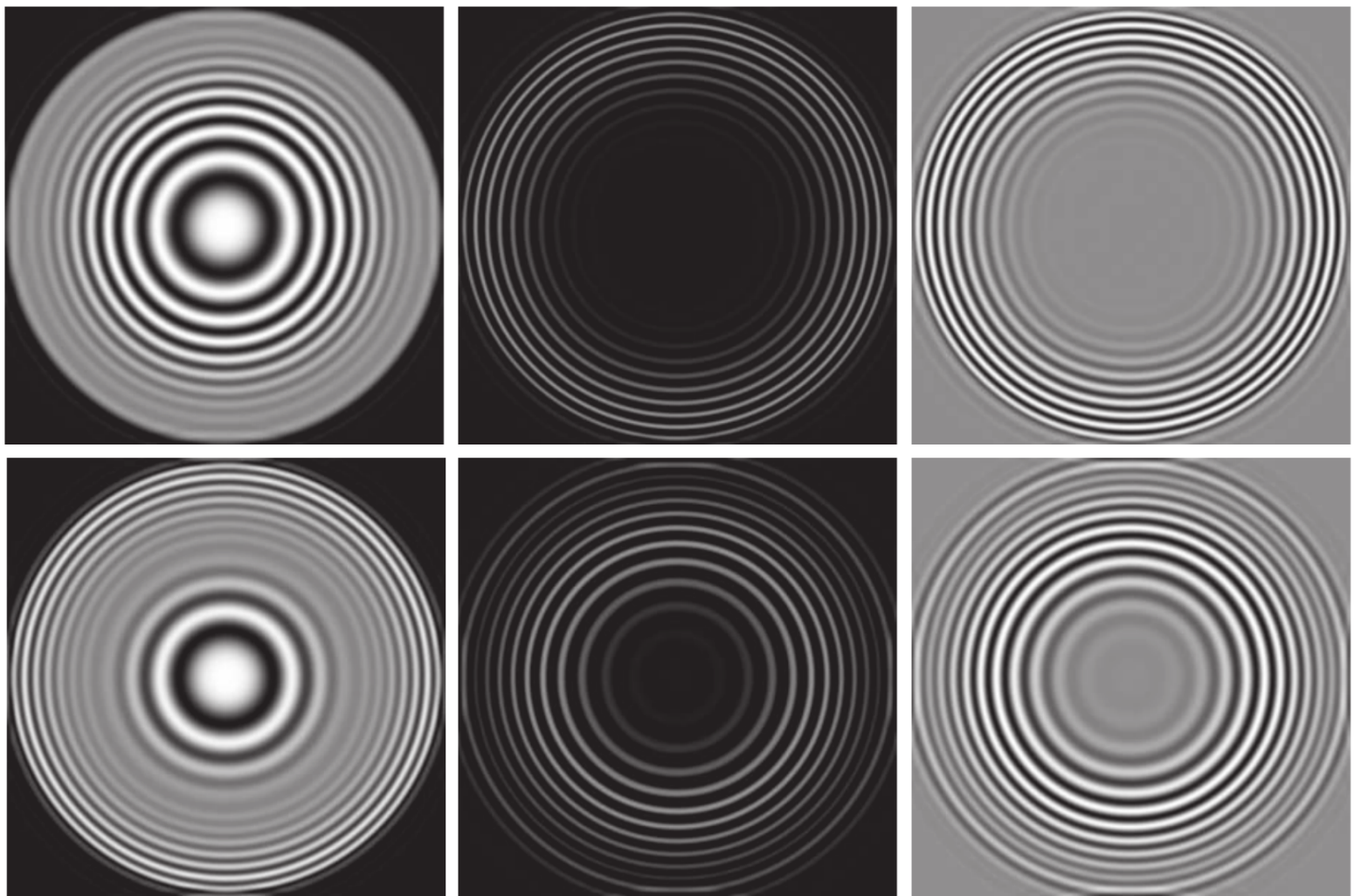
61/64

a b

FIGURE 3.55

- (a) Zone plate image filtered with a separable lowpass kernel.
(b) Image filtered with the isotropic lowpass kernel in Fig. 3.54(b).





a b c
d e f

FIGURE 3.56

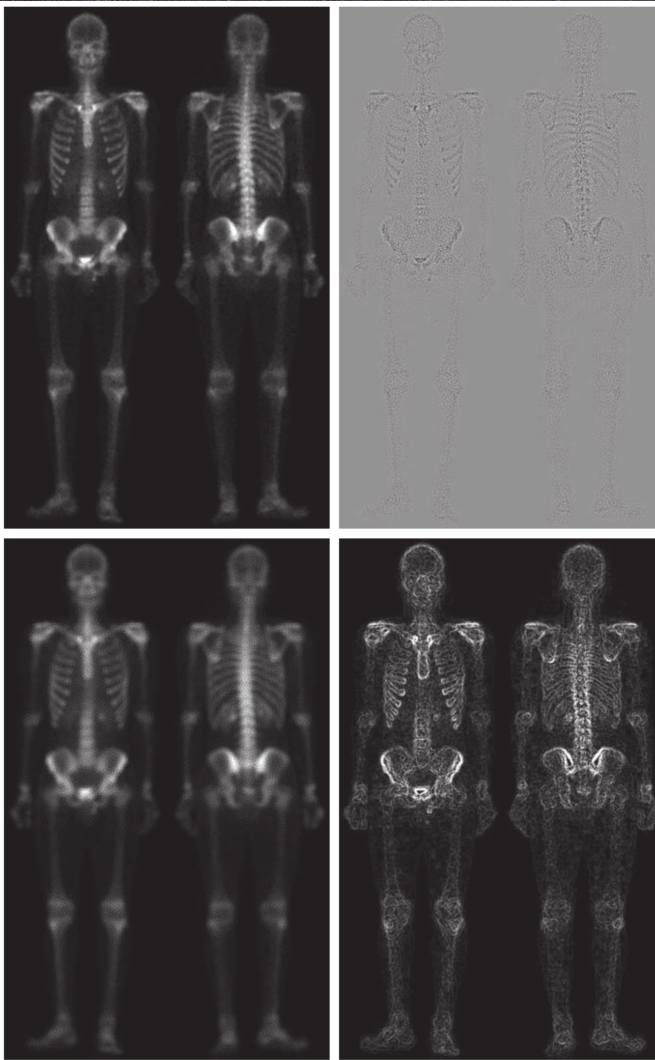
Spatial filtering of the zone plate image. (a) Lowpass result; this is the same as Fig. 3.55(b). (b) Highpass result. (c) Image (b) with intensities scaled. (d) Bandreject result. (e) Bandpass result. (f) Image (e) with intensities scaled.

空间域图像增强

a
b
c
d

FIGURE 3.57

- (a) Image of whole body bone scan.
- (b) Laplacian of (a).
- (c) Sharpened image obtained by adding (a) and (b).
- (d) Sobel gradient of image (a). (Original image courtesy of G.E. Medical Systems.)



空间域图像增强

e f
g h

FIGURE 3.57

(Continued)
(e) Sobel image smoothed with a 5×5 box filter.

(f) Mask image formed by the product of (b) and (e).

(g) Sharpened image obtained by the adding images (a) and (f).

(h) Final result obtained by applying a power-law transformation to (g). Compare images (g) and (h) with (a). (Original image courtesy of G.E. Medical Systems.)

